NRF2-related transcriptomic alterations as a long-term effect of doxorubicin treatment for childhood acute lymphoblastic leukemia

Justyna Totoń-Żurańska (justyna.toton-zuranska@uj.edu.pl)
Jagiellonian University Medical College

Joanna Sulicka-Grodzicka
Jagiellonian University Medical College

Michal Seweryn
Jagiellonian University Medical College

Ewelina Pitera
Jagiellonian University Medical College

Przemyslaw Kapusta
Jagiellonian University Medical College

Paweł Konieczny
Jagiellonian University Medical College

Leszek Drabik
Jagiellonian University Medical College

Maria Kołton-Wróż
Jagiellonian University Medical College

Bernadeta Chyrchel
Jagiellonian University Medical College

Ewelina Nowak
Jagiellonian University Medical College

Andrzej Surdacki
Jagiellonian University Medical College

Tomasz Grodzicki
Jagiellonian University Medical College

Pawel Wołkow
Jagiellonian University Medical College

Research Article

Keywords: Gene Expression and Regulation Genetics, Extracellular Vesicles, Cardiotoxicity, Doxorubicin, Basic Science Research

Posted Date: April 21st, 2021

DOI: https://doi.org/10.21203/rs.3.rs-418155/v1

Abstract

The use of doxorubicin is associated with an increased risk of acute and long-term cardiomyopathy. Despite that the number of cancer survivors is growing constantly, little is known about the transcriptional mechanisms which progress in time leading to severe cardiac outcome. It is also unclear whether long-term transcriptomic alterations are related to an acute response to doxorubicin. We have sequenced miRNA from total plasma and extracellular vesicles (EVs) from 66 acute lymphoblastic leukemia (ALL) survivors treated with doxorubicin and 61 healthy controls (254 samples in total). We identified 94 and 33 TFs regulating differentially expressed miRNA in plasma and EVs compartments, respectively. For total plasma we found: HEY1, NRF2, HIF1A, NOTCH1, and for EVs: TGFB, ZEB1, ASCL2, PELP1, SIP1, TWIST1. Analysis of the data from patients with dilated and idiopathic cardiomyopathy revealed similarities with our data from EVs, especially in the activity of TFs related to epithelial-to-mesenchymal transition (EMT). To verify if similarities exist between acute and long-term response to doxorubicin, we performed experiments on cultured as well as we studied the role of NRF2, previously considered as an important player in acute response, in transcriptomic network upon doxorubicin treatment). KEGG analysis of miRNA targets for EVs indicates development of cardiomyopathy, whereas among GO process we found terms related to cardiac septum. In vitro experiments revealed that NRF2 is co-regulated with NOTCH effectors from HEY family, with known role in muscle regeneration. NRF2 and doxorubicin treatment contribute also to the dysregulation of TWIST family, important for the process of EMT.

Introduction

Anthracyclines, including doxorubicin, have contributed to improved survival in childhood acute lymphoblastic leukemia (ALL) from less than 10–90% and are still the most widely used antineoplastic drugs worldwide[1,2]. However, because of the lack of specificity for cancer cells, anthracyclines can also damage healthy, non-cancer cells, causing severe complications including cardiotoxicity during chemotherapy, as well as many years after treatment cessation. Lipschultz et al. proved that more than 50% of doxorubicin-treated ALL survivors exhibit abnormalities of left ventricular afterload or heart muscle contractility[3] several years after treatment cessaation. Moreover, heart disease is the most common non-cancer related cause of death among cancer survivors. The central dogma of anthracyclines evoked cardiomyopathy, based on acute doxorubicin action, points to oxidative stress caused by excessive amounts of reactive oxygen species (ROS) produced due to severe functional disruption of mitochondria[4,5]. Doxorubicin action involves also massive DNA damage including 8-oxoguanine formation, DNA intercalation, and topoisomerase 2 poisoning, with downstream double-strand breaks (DSBs) formation[6–8]. As DNA lesions are repaired only partially[7], these should have consequences at the transcriptomic level and may be considered as the cause of long-term treatment side effects manifested at distant time points. However, knowledge on long-term transcriptomic processes leading to health complications due to anthracycline use is very limited, despite the fact that the number of cancer survivors is constantly increasing[9]. Furthermore, studying the molecular aspects of doxorubicin action is mostly confined to acute effects or eventually short-term studies in cultured

cardiomyocytes or animals. Thus, it is still not clear whether acute transcriptomic alterations are related to long-term effects that are linked to cardiomyopathy development.

Here, we build our approach based on the assumption that doxorubicin-induced dysregulation of the transcriptional network in target cells is responsible for sustained long-term side effects of anthracyclines. As the analysis of TF expression or activity in cardiac tissues is not feasible in human subjects, we aim to analyze the product of TF activity – miRNAs, secreted into the extracellular environment, which provides a potential for investigating the processes occurring in cells.

The latest reports on the role of extracellular vesicles (EVs) in intercellular communication underscore the stability of miRNAs in EVs and its usefulness as indicators of diverse processes[10]. Additionally, the selective characteristic of miRNA sorting into EVs and the specificity of EVs targeting due to the presence of particular surface proteins interacting with the membrane of recipient cell[11–13] were reported to reflect processes ongoing in tissues. Therefore, we searched for regulators (transcription factors (TFs) and miRNA) of the gene expression network that could be related to the development of cardiac complications in acute lymphoblastic leukemia survivors using information on miRNA expression in two compartments, namely the total plasma and EVs. On the other hand, we aimed to check whether the common denominator for long-term and acute doxorubicin transcriptomic effects exists. Thus, we analyzed transcriptomic data from experiments on cultured cardiomyocytes also in cells with downregulated NRF2, which we found as dysregulated in ALL survivors.

Results

The summary of the first part of the study regarding long-term effects of doxorubicin use is presented in Fig. 1.

Characteristics of the studied groups

There was no statistically significant difference in sex and there was a borderline nonsignificant difference in age between the study groups (as presented in Supplementary Table 1). Subsequently, we used the results of complete blood count and lipid panel tests to compare the two study groups. We applied a feature selection algorithm based on cross-validation (see Methods section) to identify variables with the largest discriminative power and subsequently tested for significance. These results are summarized in Supplementary Table 2.

Extracellular vesicles characteristics

Western blot experiments showed significant enrichment for tetraspannins CD63, CD81, and CD9 (Fig. 2). Measurements on Nanosight instrument revealed that median of vesicles size was 69,75 (Q1 = 65,05 and Q3 = 73,35) and concentration 9,17E + 12 (Q1 = 5,58E + 12 and Q3 = 1,42E + 13)

Differential expression of miRNAs in blood plasma and exosomes

We sought to find miRNAs that were differentially expressed between cases and controls in blood plasma and EVs separately. Due to an insufficient RNA amount, several samples were not included in sequencing. All further analyses were performed on 59 controls and 61 ALL patients.

We detected the following: (A1) 201 miRNAs that were differentially expressed between ALL cases versus controls in blood plasma; and (A2) 49 miRNAs that were differentially expressed in exosomes (top 10 results are presented in Table 1, the full list of differentially expressed miRNAs is available as Supplementary Table 3 (A1) and 4 (A2).

Table 1
Top 10 differentially expressed miRNAs between controls and ALL survivors in plasma (top panel - A1) and extracellular vesicles (bottom panel – A2).

A1					
miRNA	**Precursor**	**logFC**	**logCPM**	**PValue**	**FDR**
miR-184	mir-184	-5.358	8.897	2.49E-16	4.95E-13
miR-324-5p	mir-324	-3.276	1.897	4.62E-10	4.59E-07
miR-4753-5p	mir-4753	-3.149	1.352	2.08E-09	1.05E-06
let-7g-5p	let-7g	-0.701	13.642	2.11E-09	1.05E-06
miR-579-5p	mir-579	-3.385	1.968	4.17E-09	1.66E-06
miR-1-3p	mir-1-2	-2.993	7.536	6.95E-09	2.16E-06
miR-1-3p	mir-1-1	-2.973	7.480	7.61E-09	2.16E-06
miR-3140-3p	mir-3140	-3.108	1.629	1.88E-08	4.67E-06
miR-3939	mir-3939	-2.335	1.270	2.82E-07	6.21E-05
miR-1273c	mir-1273c	4.799	3.364	4.13E-07	8.21E-05
A2					
miRNA	**Precursor**	**logFC**	**logCPM**	**Pvalue**	**FDR**
miR-221-5p	mir-221	3.766	4.657	3.26E-11	6.48E-08
miR-199a-3p	mir-199a-2	1.722	9.299	9.30E-10	4.63E-07
miR-199b-3p	mir-199b	1.722	9.298	9.31E-10	4.63E-07
miR-199a-3p	mir-199a-1	1.722	9.298	9.32E-10	4.63E-07
miR-203a-3p	mir-203a	3.924	5.776	1.45E-09	5.77E-07
miR-574-5p	mir-574	3.101	3.979	1.48E-08	4.89E-06
miR-148a-5p	mir-148a	-2.639	5.911	2.00E-08	5.68E-06
miR-200a-3p	mir-200a	2.288	8.178	2.78E-08	6.89E-06
miR-145-5p	mir-145	6.219	4.239	3.27E-08	7.21E-06
miR-378i	mir-378i	1.891	6.074	1.07E-07	2.13E-05

KEGG enrichment analysis

We then performed the KEGG pathway analysis for the target genes of A1 and A2. The results of this analysis are presented in Figs. 3 and 4. Not surprisingly, a higher number of enriched terms were found for the (A1) set. Interestingly, among the top 15 significant pathways in each case, many were either

related to cardiomyopathy or strongly associated with it. Among the enriched pathways, we found tyrosine kinases, MAPK, ErbB, and neurotrophin signaling, which have been previously linked to heart function or anthracycline action[22–27]. However, only in the case of A2 analysis the term “dilated cardiomyopathy” appeared. These findings ensured us that transcriptomic changes, which in a long perspective lead to cardiomyopathy development, can be seen as early as at the time point when no severe symptoms are clinically manifested. This also suggested that miRNA in EVs may have particularly significant meaning.

GO term enrichment analysis of targets of differentially expressed miRNAs

Next, for the two sets of differentially expressed miRNAs defined above, we performed GO term enrichment analysis. Briefly, we first mapped the miRNAs to targets, subsequently annotated targets to GO terms, and performed enrichment tests. For the miRNAs in the (A1) set, we detected over 600 enriched terms, whereas for (A2), we detected over 500 enriched terms (with FDR < 0.05). The most enriched terms in (A1) included processes associated with neural and epithelial cell development, mesenchymal cell differentiation, and histone modifications. The terms most enriched in (A2) included renal, kidney, and respiratory system development as well as regulation of mRNA splicing and cardiac septum development. (Supplementary Table 5).

Association of circulating extravesicular miRNAs with interventricular septum thickness

Detailed echocardiographic examination was performed for a subset of ALL survivors. We decided to gain further insight into the association between the circulating miRNAs and the thickness of the interventricular septum (IVS), which was present among GO terms related to the A2 subset. For this purpose, we performed an association analysis of miRNAs (in EVs) versus the measured thickness of the IVS. The results are summarized in Table 2. Mir-323, mir-134, and mir-199a were previously reported as differentially expressed in patients with chronic heart failure at early stages characterized by reduced catecholamine sensitivity[28].

Table 2
Top 10 miRNAs (sorted by FDR) with expression in EVs associated with thickness of IVS in ALL survivors.

Genes	logFC	logCPM	PValue	FDR
miR-485-3p	-4.313	5.497	1.63E-07	0.0002
miR-134-5p	-4.041	6.739	1.52E-06	0.0010
miR-7110-3p	-7.648	1.350	1.83E-06	0.0010
miR-199a-5p	-4.652	7.748	6.98E-06	0.0025
miR-335-3p	-3.793	5.557	7.70E-06	0.0025
miR-485-5p	-2.912	5.075	1.55E-05	0.0043
miR-382-5p	-3.283	7.177	2.78E-05	0.0066
miR-323b-3p	-3.251	5.163	3.65E-05	0.0070
miR-409-3p	-3.220	9.400	3.80E-05	0.0070
miR-543	-2.999	7.654	5.80E-05	0.0096

Association of miRNA-specific regulatory variants with CHF.

Since we were investigating the long-term effects of chemotherapy – in particular, its relation to the cardiotoxicity of anthracyclines – therefore, we asked whether there exist common regulatory variants which are associated with the expression of A1 and/or A2 miRNAs and, at the same time, were found to be linked to HD. This analysis allows us to further prioritize the molecular pathways which may lead (in a long time horizon) to heart failure. To this aim, we used two external datasets: (1) the recent CHF GWAS results[29] and (2) miRNA eQTLs identified by the Huan et al[30]. For the miRNAs found in A1 and A2 (separately), we searched for cell-type adjusted eQTLs and subsequently queried the CHF GWAS results to find the relevant variants. For the A1 set, we were only able to find variants with signals for two miRNAs: mir-100 and mir-339, whereas for the A2 set we only identified relevant variants in mir-31.

Enrichment analysis of TFs

Next, we assessed which TFs are enriched as regulators of differentially expressed miRNAs. This analysis was performed using TransmiR v2.0 software[31]. Top results for miRNAs in A1 and A2 are presented in Tables 3 and 4. Full list of TFs available in Supplementary files (Supplementary Tables 6 and 7). In A1, we found p53 and other TFs related to its pathway, which were previously linked to DNA damage and oxidative stress also upon doxorubicin treatment[32–34], as well as NOTCH1. The second most significant TF is HEY1 involved in cardiac septum development[35]. We also found NRF2 and other TFs that are associated with short-term response to environmental stress (for instance, xenobiotics), e.g., HIF1A expression is directly regulated by NRF2[36]. In the A2 analysis, we found TFs related to epithelial-to-

mesenchymal transition (EMT) regulation: TGFB1, ZEB2, ASCL2, PELP1, SIP1, TWIST1, SLUG (SNAI2), JAG1.

Table 3
List of TFs regulating the expression of miRNAs differentially expressed in plasma between ALL survivors and healthy controls in plasma (A1 subset) (FDR < 0.05

Term	Count	Percent	P-value	FDR
E2F1	107	11.44%	1.60E-07	5.35E-05
HEY1	99	11.83%	2.40E-07	5.35E-05
PHF8	100	11.55%	6.80E-07	1.00E-04
NFE2	83	12.41%	1.43E-06	1.58E-04
KLF1	91	11.74%	2.62E-06	2.32E-04
RELA	99	11.17%	4.82E-06	3.55E-04
STAT1	101	10.93%	9.53E-06	6.02E-04
MBD3	92	11.33%	1.10E-05	6.06E-04
HIF1A	115	10.27%	1.39E-05	6.84E-04
ELF1	95	11.01%	2.27E-05	7.18E-04
ERG	118	10.09%	1.97E-05	7.18E-04
MAX	128	9.73%	1.90E-05	7.18E-04
MYC	119	10.03%	2.27E-05	7.18E-04
RUNX1	117	10.16%	1.71E-05	7.18E-04
ZNF143	92	11.12%	2.50E-05	7.36E-04
KMT2D	75	11.94%	3.47E-05	9.59E-04
CTCFL	94	10.90%	4.19E-05	1.09E-03
GATA3	99	10.67%	4.65E-05	1.14E-03
E2F6	86	11.20%	5.58E-05	1.30E-03
EP300	122	9.74%	7.25E-05	1.45E-03
KDM5B	112	10.09%	7.11E-05	1.45E-03
LARP7	96	10.68%	7.53E-05	1.45E-03
SUPT5H	75	11.68%	7.53E-05	1.45E-03
EGR1	90	10.91%	8.22E-05	1.51E-03
BRD3	51	13.49%	8.63E-05	1.53E-03
EBF1	68	12.04%	9.28E-05	1.58E-03

Term	Count	Percent	P-value	FDR
NRF1	76	11.53%	9.97E-05	1.63E-03
KLF11	62	12.40%	1.06E-04	1.68E-03
NFE2L2	30	16.85%	1.31E-04	2.00E-03
TFAP2A	89	10.80%	1.45E-04	2.13E-03
TCF12	97	10.48%	1.50E-04	2.14E-03
CCNT2	38	14.84%	1.66E-04	2.30E-03
KDM2B	97	10.43%	1.81E-04	2.42E-03
GATA1	85	10.87%	2.08E-04	2.70E-03
IRF1	75	11.26%	2.60E-04	3.19E-03
TAF1	95	10.42%	2.58E-04	3.19E-03
AR	112	9.80%	3.36E-04	3.88E-03
ARNTL	86	10.68%	3.43E-04	3.88E-03
CTCF	114	9.74%	3.27E-04	3.88E-03
ETS1	75	11.11%	4.02E-04	4.44E-03
YY1	84	10.66%	4.86E-04	5.24E-03
CEBPD	30	15.38%	5.55E-04	5.59E-03
E2F4	52	12.41%	5.37E-04	5.59E-03
WDR5	84	10.62%	5.56E-04	5.59E-03
CDK9	63	11.52%	7.10E-04	6.98E-03
ZBTB7A	62	11.55%	7.61E-04	7.31E-03
CBFB	49	12.41%	8.56E-04	8.05E-03
LDB1	19	18.63%	9.16E-04	8.43E-03
GATA2	57	11.73%	9.97E-04	9.00E-03
KLF5	38	13.33%	1.20E-03	1.06E-02
TAL1	86	10.31%	1.22E-03	1.06E-02
MXI1	75	10.67%	1.42E-03	1.18E-02
NR2C2	16	19.75%	1.39E-03	1.18E-02
TBP	79	10.51%	1.45E-03	1.19E-02

Term	Count	Percent	P-value	FDR
CXXC1	68	10.95%	1.49E-03	1.20E-02
MED1	85	10.25%	1.65E-03	1.28E-02
RARA	63	11.15%	1.65E-03	1.28E-02
FLI1	89	10.11%	1.71E-03	1.31E-02
BHLHE40	60	11.28%	1.77E-03	1.32E-02
TRIM28	94	9.94%	1.89E-03	1.39E-02
NFKB1	42	12.54%	1.93E-03	1.40E-02
GMEB2	12	22.64%	2.10E-03	1.47E-02
NCOR2	12	22.64%	2.10E-03	1.47E-02
NOTCH1	84	10.19%	2.22E-03	1.53E-02
SP1	96	9.83%	2.32E-03	1.58E-02
SUMO2	77	10.41%	2.40E-03	1.61E-02
CREB1	93	9.88%	2.55E-03	1.66E-02
TFAP4	74	10.50%	2.53E-03	1.66E-02
MYB	69	10.65%	2.84E-03	1.80E-02
RUNX3	74	10.45%	2.86E-03	1.80E-02
CHD2	58	11.13%	3.00E-03	1.87E-02
FOXO1	53	11.40%	3.10E-03	1.90E-02
STAG1	66	10.73%	3.14E-03	1.90E-02
SIN3A	79	10.22%	3.36E-03	2.01E-02
BRD4	106	9.47%	3.49E-03	2.06E-02
ELF3	36	12.72%	3.55E-03	2.06E-02
SETD1A	56	11.13%	3.70E-03	2.13E-02
HNF4A	36	12.63%	3.96E-03	2.24E-02
HNF4G	27	13.92%	4.12E-03	2.30E-02
NELFE	50	11.39%	4.38E-03	2.42E-02
CDK8	44	11.73%	4.90E-03	2.68E-02
PBX3	50	11.29%	5.23E-03	2.82E-02

Term	Count	Percent	P-value	FDR
FOS	67	10.42%	5.93E-03	3.14E-02
GABPA	77	10.08%	5.99E-03	3.14E-02
TP53	60	10.70%	6.04E-03	3.14E-02
MYCN	75	10.11%	6.54E-03	3.36E-02
JUN	71	10.22%	6.90E-03	3.43E-02
KMT2A	66	10.39%	6.87E-03	3.43E-02
TCF3	95	9.56%	6.87E-03	3.43E-02
TFAP2C	81	9.89%	7.33E-03	3.60E-02
JUND	81	9.87%	7.85E-03	3.77E-02
NR2F2	52	10.95%	7.75E-03	3.77E-02
CEBPB	87	9.65%	9.60E-03	4.56E-02
FGFR1	58	10.53%	1.01E-02	4.73E-02

Table 4
List of TFs regulating the expression of miRNAs differentially expressed in EVs between ALL survivors and healthy controls in EVs (A2 subset) (FDR < 0.05)

Term	Count	Percent	P-value	FDR
TGFB1	12	38.71%	0.00E + 00	1.48E-08
ZEB2	7	53.85%	1.20E-07	2.40E-05
ASCL2	5	100.00%	1.13E-06	8.90E-05
PELP1	5	100.00%	1.13E-06	8.90E-05
SIP1	5	100.00%	1.13E-06	8.90E-05
TWIST1	7	30.43%	2.69E-06	1.77E-04
DNMT1	6	35.29%	7.47E-06	4.20E-04
HDAC4	6	31.58%	1.27E-05	6.24E-04
SLUG	4	100.00%	1.54E-05	6.73E-04
BMP4	4	80.00%	2.72E-05	1.07E-03
SNAI1	5	35.71%	4.47E-05	1.60E-03
GTF2I	22	5.08%	1.07E-04	3.53E-03
FOXF2	3	100.00%	2.10E-04	6.37E-03
AKT2	3	75.00%	3.62E-04	8.92E-03
EED	5	21.74%	3.24E-04	8.92E-03
NFKB1	18	5.37%	3.47E-04	8.92E-03
KLF2	3	60.00%	5.70E-04	1.25E-02
SIX1	3	60.00%	5.70E-04	1.25E-02
KLF4	9	8.18%	1.08E-03	2.23E-02
TEAD4	23	4.10%	1.73E-03	3.40E-02
DDX6	2	100.00%	2.95E-03	3.64E-02
IFNB1	2	100.00%	2.95E-03	3.64E-02
IFNG	2	100.00%	2.95E-03	3.64E-02
JAG1	2	100.00%	2.95E-03	3.64E-02
KLF8	2	100.00%	2.95E-03	3.64E-02
MUC1	2	100.00%	2.95E-03	3.64E-02

Term	Count	Percent	P-value	FDR
N1ICD	2	100.00%	2.95E-03	3.64E-02
PLK1	2	100.00%	2.95E-03	3.64E-02
REL	2	100.00%	2.95E-03	3.64E-02
RREB1	2	100.00%	2.95E-03	3.64E-02
SPRR2A	2	100.00%	2.95E-03	3.64E-02
SRC	2	100.00%	2.95E-03	3.64E-02

Co-expression between differentially expressed miRNAs and selected TFs

To further investigate the association of differentially expressed miRNAs and TFs, we expanded our analysis and tested whether, for selected TFs, we observed a strong mutual relationship between the extracellular content of the differentially expressed miRNAs and the expression of a given TF in leukocytes derived from peripheral blood. For this purpose, we used the data available in the Framingham Heart Study cohort for individuals in the Offspring Cohort. For most of the selected TFs, we found that differentially expressed miRNAs were strongly co-expressed with them. For this analysis, we considered only the top 0.25% of all miRNAs as being strongly co-expressed with a given TF. We used this approach instead of the standard notion of statistical significance, as we wished to present this result only as a proof-of-principle, thus avoiding the extensive multiple testing correction. For each TF of interest, we present in Supplementary Table 8a list of co-expressed miRNAs that are in A1 and A2. Additionally, for each set of differentially expressed miRNAs (A1 and A2), we rank the miRNAs by the number of TFs co-expressed with them (Table 5). Interestingly, two miRNAs correlated with the highest number of TFs are involved in NRF2 pathway through targeting NRF2 inhibitors (miR-193a – targets NRF2 antagonist BACH2[37,38], miR-141 - NRF2 repressor KEAP1[39]. Additionally, our analysis of FHS data also shows the correlation of NRF2 with the high number of miRNAs differentially expressed in ALL survivors.

Table 5

Differentially expressed miRNAs (separately in sets A1 and A2) ranked by the number of co-expressed TFs (out of the TFs selected for the analysis). mRNA expression in peripheral blood leukocytes was measured by microarray assays, and the expression of miRNA was determined by RNA sequencing.

A1		A2	
miRNA	**no of co-expressed TFs**	**miRNA**	**no of co-expressed TFs**
miR-193a	15	**miR-31**	14
miR-141	13	**miR-141**	13
miR-190a	12	**miR-203a**	10
miR-210	9	**miR-221**	9
miR-579	9	**miR-369**	9
miR-877	9	**miR-21**	8
miR-95	8	**miR-361**	8
let-7f-2	7	**miR-629**	8
miR-29c	7	**miR-145**	6
miR-642a	7	**miR-1301**	5
let-7f-1	6	**miR-199b**	5
miR-100	3	**miR-500a**	3
miR-324	3	**miR-10b**	2
miR-339	3	**miR-200a**	2
miR-500a	3	**miR-215**	2
miR-584	3	**miR-4446**	2
miR-942	3	**miR-1180**	1
let-7i	2	**miR-148a**	1
miR-4446	2	**miR-23b**	1
miR-769	2		
let-7g	1		
miR-1229	1		
miR-144	1		
miR-34a	1		

A1	A2
miR-4433a	1

Comparison with TFs enriched in regulation of miRNAs associated with cardiomyopathy.

To assess whether our data on circulating miRNAs reflect processes active in people with dilated cardiomyopathy (DCM) or idiopathic cardiomyopathy (ICM), which are manifested by changes in their circulating and/or target tissue miRNAs, we analyzed the data of Akat et al[40]. First, we compared the differentially expressed miRNAs in A1 and A2 sets with miRNAs differentially expressed between the serum of healthy individuals (HC) and patients with DCM/ICM (prior to any surgical intervention). We obtained the following results: 14 miRNAs in A1 that were also differentially expressed between HC and ICM in blood plasma; 13 miRNAs in A1 that were also differentially expressed between HC and DCM; 14 miRNAs in A2 that were also differentially expressed between HC and ICM; and 8 miRNAs in A2 that were also differentially expressed between HC and DCM. Of these, 9 miRNAs were common between ICM and DCM for A1 subset and 4 were common between ICM and DCM for A2 subset (Table 6, Fig. 5). Second, we performed an analysis of TF enrichment on the results of differential miRNA expression between HC and DCM/ICM (we used the TransmiR software as in the case of our in-house data). The results are available in Tables 7 and 8. We found 5 of 9 significant TFs related to the expression of circulating miRNAs in ICM patients present among the top significant TFs in EVs (A2 subset) Of particular interest were important EMT regulators: TGFB, ZEB1, SNAI1, and TWIST. Additionally, all 3 significant TFs in DCM were present in either A1 or A2. Results are presented in Fig. 6. Subsequently, we analyzed the tissue mRNA expression data from the same study. Again, we considered only samples from HC, DCM, and ICM (excluding the fetal hearts from the analysis). We identified two sets of differentially expressed probes (under FDR < 0.05) – between HC and DCM as well as between HC and ICM. Subsequently, we used the “RcisTarget” package to evaluate the enriched motifs of TF binding in 50-kb window around the differentially expressed genes. Among the significant TFs, we found that many were present in our data from ALL survivors, for instance, NFE2, STAT1, STAT5A, NFKB, EP300, GATA1, GATA2, and GATA3 (data not presented).

Table 6
The list of miRNAs common for A1 or A2 analyses and ICM/DCM datsets

Group	Common DE miRNA
HC/ICM and A1 analysis	hsa-mir-208b, hsa-mir-3680, hsa-mir-202, hsa-mir-101, hsa-mir-769, hsa-mir-511, hsa-mir-181b, hsa-mir-216a, hsa-mir-210, hsa-mir-3158, hsa-mir-584, hsa-mir-455, hsa-mir-95, hsa-mir-1277
HC/DCM and A1 analysis	hsa-mir-1, hsa-mir-208b, hsa-mir-144, hsa-mir-194, hsa-mir-511, hsa-mir-181b, hsa-mir-216a, hsa-mir-210, hsa-mir-3158, hsa-mir-584, hsa-mir-455, hsa-mir-193a, hsa-mir-95
HC/ICM and A2 analysis	hsa-mir-199b, hsa-mir-148a, hsa-mir-200a, hsa-mir-361, hsa-mir-429, hsa-mir-21, hsa-mir-132, hsa-mir-15b, hsa-mir-215, hsa-mir-200b, hsa-mir-197, hsa-mir-10b, hsa-mir-29a, hsa-mir-143
HC/DCM and A2 analysis	hsa-mir-148a, hsa-mir-369, hsa-mir-1, hsa-mir-15b, hsa-mir-215, hsa-mir-1180, hsa-mir-31, hsa-mir-29a

Table 7
List of significantly enriched transcription factors which regulate differentially expressed miRNAs between ICM patients and controls in blood plasma.

Term	Count	Percent	Fold	P-value	Bonferroni	FDR
GTF2I	48	11,09%	2,1	9,00E-08	3,99E-05	2,00E-05
TGFB1	13	41,94%	7,94	8,00E-08	3,66E-05	2,00E-05
ZEB2	7	53,85%	10,2	2,94E-05	1,28E-02	4,26E-03
SNAI1	7	50,00%	9,47	4,23E-05	1,84E-02	4,60E-03
TWIST1	8	34,78%	6,59	9,18E-05	3,99E-02	7,98E-03
STAT5	7	35,00%	6,63	2,52E-04	1,09E-01	1,82E-02
AKT1	4	80,00%	15,15	6,19E-04	2,69E-01	3,84E-02
MYOG	4	66,67%	12,63	9,92E-04	4,31E-01	4,79E-02
NF-Y	4	66,67%	12,63	9,92E-04	4,31E-01	4,79E-02
AP-1	5	38,46%	7,29	1,46E-03	6,36E-01	5,43E-02
CUX1	8	21,62%	4,1	1,39E-03	6,07E-01	5,43E-02
TNFSF12	4	57,14%	10,82	1,50E-03	6,52E-01	5,43E-02

Table 8
List of significantly enriched transcription factors which regulate differential miRNAs differentially expressed between DCM patients and controls in blood plasma.

Term	Count	Percent	Fold	P-value	Bonferroni	FDR
GTF2I	67	15,47%	2,2	0,00E + 00	1,73E-08	1,73E-08
HNF4A	37	12,98%	1,84	2,24E-04	9,49E-02	3,16E-02
TGFB1	10	32,26%	4,58	2,10E-04	8,90E-02	3,16E-02

Transcription factors co-expression in cardiomyocytes

With the results given above, we hypothesized that NRF2, important for short-term response to doxorubicin, might play also a significant role in the development of cardiomyopathy. Therefore, we decided to study NRF2 function in terms of its co-expression network. The schematic view of this part of study is depicted in Fig. 7.

To verify the functional effects of NRF2 on the transcriptional response to doxorubicin in human cardiomyocytes, we performed silencing experiments on immortalized cardiomyocytes (IHC). Subsequently, we identified four sets of differentially expressed mRNAs: B1 – between shCTRL and shNRF2 cells with no dox treatment, B2 – between shCTRL and shNRF2 cells with dox treatment, B3 – between no-dox and dox treatment in shCTRL cells, B4 - between no dox and dox treatment in shNRF2 cells. The results of these comparisons are summarized in Supplementary Tables 9–12. Due to the limited sample size, we did not focus on the direct interpretation of these results, instead, we performed a transcription factor enrichment analysis based on the ChEA3 tool. In this way, we aimed to gain further insight in the mutual relations of the TFs with NRF2 in the context of dox treatment. For each of the sets B1-B4, we used the top 50 differentially expressed mRNAs and obtained scores for TFs which are likely to be regulating these mRNAs. We decided to use only the top 50 mRNAs as we wanted to avoid the bias associated with the different numbers of differentially expressed genes between the considered conditions. The complete results of this analysis are summarized in Supplementary Tables 13–16. Subsequently, we detected the TFs with the largest fold changes between the study conditions. In other words, we identified four sets of TFs: T1 – with the highest (positive) fold change between scores for B1 and B2; T2 – with the lowest (negative) fold change between scores for B1 and B2; T3 – with the highest (positive) fold change between scores for B3 and B4; T2 – with the lowest (negative) fold change between scores for B3 and B4. Therefore, the set T1 represents TFs likely to be regulating B2 and not B1 mRNAs, T2 – TFs likely to be regulating B1 and not B2 mRNAs, T3 – TFs likely to be regulating B4 and not B3 mRNAs, T4 – TFs likely to be regulating B3 and not B4 mRNAs. Results are summarized in Table 9 and in Supplementary Tables 17–20.

Table 9
List of top 10 TFs regulating differentially expressed transcripts in T1-T4 comparisons (D0 – cells without doxorubicin, D1 – cells treated with doxorubicin, CTRL – control cells for NRF2 silencing experiments, shNRF2 – cells with down-regulated NRF2 expression).

D0 vs D1 specific transcription factors (T1)			
name	logFC	scoreD0	scoreD1
TBX3	-2,2449999	455,5	48,25
ARNT2	-1,7061109	282,7	51,33
ARHGAP35	-1,6882678	1339	247,5
ZNF275	-1,6795578	1078	201
FOXD1	-1,6190569	679	134,5
PPARG	-1,4752618	232,6	53,2
PBX1	-1,4635631	468	108,3
SOX5	-1,3442327	703	183,3
MEIS3	-1,3271333	272,7	72,33
SOX8	-1,2507284	316,7	90,67
D1 vs D0 specific transcription factors (T2)			
name	logFC	scoreD0	scoreD1
GCM2	1,9397355	123	855,7
AEBP1	1,8607523	35	225
IRX4	1,7549276	81,67	472,3
HEY2	1,6157733	100,7	506,7
NKX31	1,5715715	183	881
PRRX2	1,528863	125,3	578
HEYL	1,4401223	33	139,3
NKX62	1,4316223	186	778,5
ERG	1,3920915	94,6	380,6
IRF6	1,3776191	101,3	401,7
CTRL vs shNRF2 specific transcription factors (T3)			
name	logFC	scoreCTRL	scoreNRF

D0 vs D1 specific transcription factors (T1)			
CSRNP1	-3,6154123	334,5	9
NPAS4	-2,3940218	420	38,33
BPTF	-2,0298238	776,5	102
ZBTB9	-2,0105266	1197	160,3
ZNF883	-1,9484693	1565	223
JUNB	-1,9247826	140,5	20,5
JUND	-1,7189715	368,2	66
EGR3	-1,6796422	354	66
MEIS3	-1,538962	1123	241
FEV	-1,529415	387,7	84
shNRF2 vs CTRL specific transcription factors (T4)			
name	logFC	scoreCTRL	scoreNRF
FOXD1	4,1097295	21,5	1310
ZNF469	3,7344469	37	1549
RFX8	2,9623531	49,5	957,5
TWIST2	2,6523201	107	1518
PPARG	2,6224365	44,2	608,6
ATOH8	2,600565	33,33	449
FOXC2	2,4831507	95	1138
MSANTD3	2,4655637	130,5	1536
PLSCR1	2,4174399	76	852,5
TBX18	2,3973929	126,7	1393

These results show that doxorubicin treatment of control cells induces changes in the activity of several TFs containing basic Helix-Loop-Helix (bHLH): TWIST1 and 2, HIF1A, and HES1, HES4. The comparison of untreated control cells and shNRF2 cells also revealed significant alterations in the functioning of TWIST1 and TWIST2, ZEB1, SNAI1, as well as other members of the bHLH family known as NOTCH effectors- HEY2 and HEYL. Upon doxorubicin treatment, NRF2 downregulation caused significant alterations in HEY1 functioning, whereas in the comparison of shNRF treated and untreated cells we found both HEY TFs and HES1, HES6. It indicates that NRF2 downregulation and doxorubicin treatment

have common effectors including TWIST, HEY, and HES TFs which belong to the bHLH family, of which many we found to be dysregulated in ALL patients.

Co-expression of NRF2 and other TFs in the GTEx Heart Left Ventricle RNA-sequencing data

To further refine these results, for each set T1-T4, we took the top 50 TFs (Supplementary Tables 17–20) and tested the co-expression between the mRNAs of these TFs (and the NRF2 mRNA) in the GTEx Heart Left Ventricle RNA-sequencing data (for the co-expression analysis TFs with TPM > 0.5 were chosen). The results are presented in Figs. 8–11. Interestingly, in this way we were able to identify a cluster of: 13 TFs for T1, 1 TFs for T2, 29 TFs for T3 and 15 TFs for T4 which are co-regulated with NRF2 (with a correlation coefficient above 0.5). The list of TFs for each subset is presented in Table 10. Hence, both doxorubicin treatment and NRF2 deficiency cause alterations in HEY1 functioning. Doxorubicin treatment of NRF2 deficient cells causes changes in the functioning of TWIST1, TWIST2, SNAI2, which could be related to the difference in GRHL1 action (T2 comparison - sh control vs sh NRF2 cells upon treatment).

Table 10
The list of TFs regulating T1-T4 subsets that are co-expressed with NRF2 in the GTEx Heart Left Ventricle RNA-sequencing data.

	T1	T2	T3	T4
TFs	CF7L1, NFE2L2, TWIST2, PPARG, ZNF718, PRDM8 ,HEY1, LHX6, NFATC4, SETBP1, TSHZ3, MEIS3, ZNF525	GRHL1	SPEN, ZNF669, FOXN2, ZNF2, CSRNP1, RBPJ, ZNF322, ZKSCAN3 ,ZBTB2, HEY1, MYC, KLF9, ZBTB6, KLF6, ZNF778, BPTF, ZNF24, SETBP1, ADNP2, JUNB, JUND, ZNF529, ZNF112, MEIS3, ZNF175, EBF4, PLAGL2, ZNF74, ZXDB	PRRX1, OSR1, ATOH8, NFE2L2, TWIST2, PPARG, PLSCR1, MECOM, TBX18, TWIST1, SNAI2, NFATC4, FOXC2, TSHZ3, ETS2.

Discussion

Here we present diverse lines of evidence that long-term molecular effects of doxorubicin action in ALL survivors include persistently altered transcription factor activity, which results in changes of miRNA presence in the circulation that may contribute to cardiomyopathy development, the major life-threatening long-term effects of anthracycline treatment[41,42]. We demonstrate that especially miRNA circulating in EVs may be a useful source of information on transcriptomic processes that are changed due to anticancer treatment.

Indeed, our KEGG and GO enrichment analyses for differentially expressed vesicular miRNA targets indicate that processes including dilated cardiomyopathy and related processes (e.g. ERBB signalling[43,44]) are ongoing in ALL survivors. Hence, we decided to search for TFs that regulate the expression of differentially expressed miRNAs.

Among TFs regulating miRNAs in EVs, we found multiple important players in EMT - TGFB1, SLUG, JAG1, SNAI1, ZEB-1, SIP-1, TWIST, and BMP4[45–49]. TGFB1, having the highest statistical significance, was reported to be a master regulator of EMT [50,51], a process linked to therapy-triggered senescence[52] and fibrosis[53,54]. Senescence, proposed as an alternative to entering apoptosis in response to genotoxic treatment[55,56], is also suggested to reinforce long-term cardiac complications of anticancer treatment[57]. It is noteworthy that TGFB expression can be increased in the heart tissue many weeks after doxorubicin treatment[58].

Moreover, TGFB1- related factors including TWIST1 and SLUG (SNAI2), were previously reported as related to cardiac morphogenesis including atrioventricular cushion formation or cardiac septation[59,60]. Recent data revealed that TWIST2 is expressed in specific populations of interstitial heart cells, which contributes to cardiac homeostasis and regeneration[61]. Additionally, TWIST1 as well as TWIST1-regulated mir-199a (miRNA correlated with IVS thickness in our study) were reported as down-regulated in the heart tissue of patients with severe cardiomyopathy[62]. Dysfunction within this system may result in poor cell renewal and proliferation, as was shown for stem cells[63].

Additionally, our analysis of miRNA expression data from individuals with dilated and idiopathic cardiomyopathy revealed that except for some similarities in miRNA differential expression, vesicular miRNAs in the former ALL patients share Tfs regulators with miRNA related with cardiomyopathy (TGB, ZEB2, SNAI1, TWIST1).

Moreover, one of the miRNA common for these analyses, mir-31, significantly upregulated in extracellular vesicles of ALL survivors, and which we found to be involved in the genetics of heart failure is also the top miRNA correlated with the highest number of Tfs regulating miRNA in A2 analysis, including factors well known for significant role in both response to doxorubicin and cardiomyocyte functioning (NRF2, TP53, HIF1A) as well as EMT process (ZEB1, SNAI1). Mir-31 has been previously reported to be upregulated in cardiomyocytes due to hypoxia or oxidative stress and in hearts after myocardial infarction. Its silencing upregulated troponin T in cardiomyocytes, while administration of mir-31 inhibitor in rats post-myocardial infarction improved heart function[64]. Moreover, a recent paper has shown that doxorubicin treatment induced mir-31 expression in cultured cardiomyocytes as well as in heart tissue, causing downregulation of RNA binding protein quaking playing a significant role in doxorubicin-induced cardiotoxicity[65], what imply that pathways related to mir-31 might also be valuable targets for future studies.

Surprisingly, the results of our analyses support the role of NRF2 as one of the key regulators of the transcriptomic network in ALL survivors treated with doxorubicin. NRF2 is associated with doxorubicin resistance and short-term effects of chemotherapy[66,67]. Down-regulation of NRF2, which physiologically plays the main role in the protection against oxidative stress through the activation of transcription of antioxidative response genes, causes excessive doxorubicin-induced cardiotoxicity [68,69]. Additionally, prolonged oxidative stress and unbalanced NRF2 activity may induce senescence and premature age-

related diseases, which have been attributed to the long-term effects of anticancer treatment[70,71]. To investigate the detailed role of NRF2 in the transcriptional network upon doxorubicin treatment, we performed NRF2 silencing experiments on cultured cardiomyocytes. It reveals that even without drug exposure, down-regulation of NRF2 is accompanied by changes in the functioning of NOTCH1 (present also among TFs regulating plasma miRNAs) and TGFB-related TFs (present among TFs regulating miRNAs in EVs') involved in EMT: TGFB, TWIST1, TWIST2, ZEB1, SNAI2, which have been previously reported as related to cardiac morphogenesis including atrioventricular cushions formation or cardiac septation[59,60]. We also observed significant alterations of NOTCH signaling targets: HEY2, HEYL, and HES factors are required for efficient chromatin binding by HEY1[72], which we show is further dysregulated in shNRF2 cells upon doxorubicin treatment. HEY1, HEY2, and HEYL together with HES family of TFs are crucial for the formation of valves and septa during embryogenesis[59]. HEY1, the second significant TF regulating plasma miRNA expression, turns up as differentially active upon NRF downregulation as well as during doxorubicin stimulation in control cells. It was previously shown that inactivation of HEY1 and HEYL causes congenital heart defects including ventricular septal defects[35]. Whereas in aging muscle stem cells, HEY1 rescues cells from death due to mitotic catastrophe during muscle regeneration[73]. Moreover, in the case of NRF2 loss, HEY1 downregulation was accompanied by a delay in repair after chemical injury[63]. Second of Hey genes - HEY2 is specifically expressed in the interventricular septum, ventricular compact myocardium, the atrioventricular canal outflow tract, at the base of trabeculae, and in epicardial cells[74]. It was also postulated that HEY2 is necessary to maintain ventricular identity by mature cells[74]. Indeed, cardiomyocyte-specific deletion of HEY2 results in the transcription of atrial genes in the ventricular myocardium accompanied by impairment of cardiac contractility and changes in the morphology of the right ventricle[75,76], and its deficiency causes septal defects and cardiomyopathy in mice[75].

Additionally, TWIST1 as well as TWIST1-regulated mir-199a (miRNA correlated with IVS thickness in our study) were reported as down-regulated in the heart tissue of patients with severe cardiomyopathy[62]. Notably, GRHL1, a regulator of gene expression upon doxorubicin treatment in the case of diminished NRF2 activity, is a member of the grainyhead family of TFs, which acts as a suppressor of TGFβ-induced, and TWIST-induced EMT[77]. The finding of co-regulation between NRF2 activity and NOTCH signaling in ALL survivors remains in line with previous reports suggesting reciprocal regulation between these these Tfs[78]. Dysfunction within this system may result in poor cell renewal and proliferation, as was shown for stem cells[63].

Here we also show that doxorubicin treatment of cardiomyocytes alters the activity of RBPJ, an important transcriptional regulator of NOTCH[79]. Additionally, since TWIST, HEY, and HES proteins all belong to the basic helix-loop-helix (bHLH) transcription factors family[80,81], it seems reasonable to hypothesize that the co-regulation of these TFs with NRF2 may be related to the 60 amino acid region which contains two highly conserved domains, considered as involved in interactions with TFs[82].

In summary, our approach allowed to identify dysregulated mechanisms, including altered NRF2 activity, that might be involved in late cardiac complications due to doxorubicin treatment.

However, to the best of our knowledge, it is still unclear how the damage caused by anthracyclines, often during childhood, can be propagated until adulthood. Doxorubicin-induced DSBs are especially frequent around active promoters[83] and are known to cause transcriptional repression[84]. Gene expression silencing was shown to be converted to long-term stable silencing through modifications like CpGs or histone methylation, which may be heritable [85,86]. Thus, NRF2 gene with high transcriptional activity upon exposure to oxidative stress, could be at particularly high risk of modification during doxorubicin treatment. Although further investigations are required to prove such possibility.

Our approach using differential expression of circulating miRNA allowed to identify dysregulated mechanisms, which may be involved in the development of long-term consequences of doxorubicin treatment in ALL survivors. Additionally, microRNA encapsulated in extracellular vesicles significantly indicated EMT-related processes which seem to be related to cardiomyopathy development, which although needs further study.

In summary, we present data proving that NRF2-related molecular changes initiated by doxorubicin treatment may cause alterations in the functioning of transcription factors related to cardiac cells identity and regeneration. Among them, especially HEY as well as TWIST Tfs could be considered as potential targets in future studies.

Our approach using differential expression of circulating miRNA allowed to identify dysregulated mechanisms, which may be involved in the development of long-term consequences of doxorubicin treatment in ALL survivors. Additionally, microRNA encapsulated in extracellular vesicles significantly indicated EMT-related processes which seem to be related to cardiomyopathy development, which although needs further study.

Materials And Methods

Study cohort

The survivor population was recruited from the Childhood Cancer Survivorship Clinic at the University Hospital in Kraków. Informed consent was obtained in accordance with the Declaration of Helsinki. The study was approved by the Bioethics Committee at the Jagiellonian University (Approval No. 122.6120.274.2015). Eligibility criteria included the following: (1) diagnosis of ALL before 18 years of age and (2) 5 or more years since the completion of cancer treatment (doxorubicin). Exclusion criteria included the following: (1) time from the end of therapy for ALL shorter than 5 years, (2) relapse or secondary cancer at the time of the study or during the 5 preceding years. The study participants underwent a comprehensive clinical evaluation, including physical examination accompanied by anthropometric assessments. Healthy controls were recruited at the Blood Donation Center in Kraków,

Poland. Blood sampling, biochemical analyses, and echocardiographic evaluation were performed as previously[14]

Isolation and characterization of EVs

Plasma EVs were isolated with the miRCURY Exosome Isolation Kit (Exiqon, Qiagen, Aarhus, Denmark) according to the manufacturer's protocol. In line with International Society for Extracellular vesicles recommendations[15],the presence of protein markers was assessed by western blot analysis using antibodies against CD63, CD81, and CD9. Size distribution of EVs was measured by Nanoparticle Tracking Analysis with NanoSight (Malvern Panalytical, Malvern, United Kingdom).

RNA extraction and preparation of miRNA libraries

Small RNA was extracted from EVs and total plasma with miRCURY RNA Isolation Kit (Exiqon, Qiagen). Libraries were prepared with NebNext Small RNA Library Prep (New England Biolabs, Ipswich, MA, USA). Quality control steps for libraries were performed on TapeStation (Agilent Technologies, Santa Clara, CA, USA) before and after size selection. cDNA concentration was measured using the Quantus fluorometer (Promega, Madison, Wisconsin, USA). Pooled libraries were sequenced with High Output v2.0 reagents on the NextSeq 500 sequencer (Illumina, San Diego, CA, USA).

Cell culture experiments and NRF2 gene silencing

Immortalized human cardiomyocytes (IHC) (Applied Biological Materials, Vancouver, Canada) were cultured in Prigrow1 medium supplemented with 5% fetal bovine serum. IHC cells (passage No 5) were transduced with MISSION® shRNA lentiviral particles targeting NRF2 and negative control lentiviral particles targeting no known mammalian genes (Sigma-Aldrich, St. Louis, MO, USA). Two different shNRF2 lentiviral clones were used: NM_006164 / TRCN0000007558 and NM_006164 / TRCN0000007555. Cells were transduced at MOI of 2.5 and 5 in the presence of 6 µg/ml Hexadimethrine bromide (Sigma-Aldrich, St. Louis, MO, USA) according to the manufacturer's protocol. After 72h, cells were subjected to selection with 0.3 µg/ml puromycin (InvivoGen, San Diego, CA, USA) for 2 weeks. The knockdown of NRF2 expression in the obtained cell lines was verified using the qRT-PCR method. Cells seeded on 6-well culture plates were treated with 0,25uM doxorubicin for 2 h, washed with PBS, and lysed with lysis buffer.

RNA-sequencing

Total RNA was extracted from control and doxorubicin-treated cardiomyocytes using GeneMATRIX UNIVERSAL RNA Purification Kit (EURx, Gdansk, Poland). RNA quality check was performed on TapeStation (Agilent Technologies, Santa Clara, CA, USA). mRNA libraries were prepared with Sense mRNA-Seq Library prep Kit v2 (Lexogen, Vienna, Austria) according to the manufacturer's protocol. cDNA was amplified and indexed in 12 PCR cycles. Pooled libraries were sequenced on NextSeq (Illumina) using NextSeq 500/550 High Output Kit v2.0. at 1,8 pM final concentration.

Bioinformatics analysis

Raw BCL files from a NextSeq sequencing runs were demultiplexed and converted into fastq files with Illumina Bcl2Fastq v.2.20.0.422 software. Quality of the reads was checked with a FastQC software, v0.11.8[16]. For the miRNA analysis, the reads were trimmed to remove primers and poor quality bases with Cutadapt, v1.18[17]. Then, reads with length < 18 or > 30 nucleotides and reads without 3' adapter were removed. The cleaned reads were then aligned to miRBase database v22.1[18] and counted using miRDeep2 software v0.0.8[19]. Normalized miRNA read count generated from miRDeep2 was used in

Bioinformatics analysis

Raw BCL files from a NextSeq sequencing runs were demultiplexed and converted into fastq files with Illumina Bcl2Fastq v.2.20.0.422 software. Quality of the reads was checked with a FastQC software, v0.11.8[16]. For the miRNA analysis, the reads were trimmed to remove primers and poor quality bases with Cutadapt, v1.18[17]. Then, reads with length < 18 or > 30 nucleotides and reads without 3' adapter were removed. The cleaned reads were then aligned to miRBase database v22.1[18] and counted using miRDeep2 software v0.0.8[19]. Normalized miRNA read count generated from miRDeep2 was used in further analysis. The raw sequences, along with raw and normalized counts from miRDeep2 software were deposited in GEO (GSE145176). For mRNA analysis, the paired-end reads were trimmed with Cutadapt, v1.18 [17], to remove the starter/stopper heterodimer sequence accordingly to the kit manufacturer's instructions. Then, the reads were aligned reads to the reference genome GRCh38 (ensembl version 95), with STAR v.2.7.0c[20], using a two-pass method. The uniquely aligned reads mapped to genes were enumerated using HT-Seq-count v.0.11.2[21]. After quality assessment of alignment and enumerated gene expression levels, the raw expression values were uploaded into R for further analysis.

Statistical methods

All statistical analyses and filtering steps were performed in R (v3.5.2). Out of 1986, the detected miRNAs, 1452 (with at least five reads observed per sample) were considered as positive hits and were used in the statistical analysis. The differential expression was analyzed by the edgeR package with two different experimental designs: model #1. Xp ~ compartment + status:compartment and model #2. xp ~ status + compartment:status.

Additionally, the results of differential expression analysis were further filtered, and only results with FDR < 0.05 and logCPM > 1 were considered significant. Elastic net regression was performed as implemented in the package "glmnet" with default settings for cross-validation-based feature selection. GO enrichment was performed using the "topGO' package, and the KEGG enrichment analysis was performed using the RbiomirGS package. eQTL enrichment analysis was performed using Fisher's exact test. For correlation tests, Pearson's product-moment correlation coefficient was used. TransmiR v2.0 software was accessed through www.cuilab.cn.

The analysis of mRNA expression was performed by means of the edgeR package in R. In short, raw reads were normalized for library size and subsequently dispersion was estimated (common, tagwise,

and trended). For target differential expression analysis, genes with at least 10 reads in at least one sample were used. Differentially expressed genes were detected by means of the Likelihood Ratio Test in a linear model with suitably chosen contrasts.

The ChEA3 tool was used as available through. For the enrichment analysis, the top 50 differentially expressed genes were used.

Analysis of the correlation between miRNA expression and echocardiography

To test in an unbiased fashion whether the expression in plasma/exosomes of miRNA correlates with selected echocardiographic parameters, we used the following approach. Using pseudocounts, we first selected features (miRNAs) which are differentially variable between cases and controls (using Levene's test). For further analyses, we used only the ones which remain significantly differentially variable with FDR < = 0.05. Subsequently, we reduced the dimension of the data to three using the unsupervised UMAP method. We did this separately in plasma and exosomes (differentially variable miRNAs were selected regardless of compartment). In what follows, we used the LASSO model to test which echocardiographic parameters correlate with the three coordinates of the embedding (here the set of covariates is defined by the selected parameters of the echocardiographic test and the dependent variable is three-dimensional and represented by the coordinates of the UMAP embedding)

Declarations

Conflict of interest: *The authors report no conflict of interest*

Acknowledgements

The Framingham Heart Study is conducted and supported by the National Heart, Lung, and Blood Institute (NHLBI) in collaboration with Boston University (Contract Nos. N01-HC-25195 and HHSN268201500001I). This manuscript was not prepared in collaboration with investigators of the Framingham Heart Study and does not necessarily reflect the opinions or views of the Framingham Heart Study, Boston University, or NHLBI.

Additional funding for SABRe was provided by the Division of Intramural Research, NHLBI, and Center for Population Studies, NHLBI.

Funding for SHARe Affymetrix genotyping was provided by NHLBI (Contract No. N02-HL-64278). SHARe Illumina genotyping was provided under an agreement between Illumina and Boston University. The RNA expression data used for the analyses described in this manuscript were obtained from the dbGaP accession number phs000007.v23.p1.

Funding support for the Framingham Extracellular RNAs: Biomarkers for Cardiovascular Risk and Disease dataset was provided by NIH grant 1UH2TR000921-01. The data used for the analyses described in this manuscript were obtained from the dbGaP accession number phs000007.v28.p10 (dataset l_rnaxcell_ex08_1_0840s.HMB-IRB-MDS).

Sources of funding

This research was funded by the National Science Centre (Poland), grant No. 2015/17/D/NZ7/02165 (to J.T.-Ż.)

Authors Contributions:

JTZ MTS PW - contributed to conceptualization, wrote and edited this manuscript ,

MTS, P. Kapusta, LD – performed bio-nformatic and statistical analyses

MKW, EP, P. Konieczny – conducted experiments,

JSG, BC, EN - contributed to conceptualization, provided samples, and collected clinical data

AS TG - contributed to the conceptualization

All authors read and approved the final manuscript.

Ethics approval and consent to participate

The study was approved by the Bioethics Committee at the Jagiellonian University (approval No. 22.6120.274.2015).

Access to FHS was approved by the Ohio State University IRB (Protocol #2013H0096).

Data availability

The raw RNA sequences, along with raw and normalized counts from miRDeep2 software were deposited in GEO (GSE145176).

Figures 1 and 7 were prepared with BioRender tool.

References

1. *Birch, J. M., Marsden, H. B., Jones, P. H., Pearson, D. & Blair, V. Improvements in survival from childhood cancer: results of a population based survey over 30 years. Br Med J (Clin Res Ed) 296, 1372–1376 (1988).*
2. *Bonaventure, A. et al. Worldwide comparison of survival from childhood leukaemia for 1995–2009, by subtype, age, and sex (CONCORD-2): a population-based study of individual data for 89 828*

children from 198 registries in 53 countries. Lancet Haematol 4, e202–e217 (2017).

3. *Lipshultz, S. E. et al. Late Cardiac Effects of Doxorubicin Therapy for Acute Lymphoblastic Leukemia in Childhood. http://dx.doi.org/10.1056/NEJM199103213241205 https://www.nejm.org/doi/10.1056/NEJM199103213241205?url_ver=Z39.88-2003&rfr_id=ori%3Arid%3Acrossref.org&rfr_dat=cr_pub%3Dwww.ncbi.nlm.nih.gov (2010) doi:10.1056/NEJM199103213241205.*
4. *Octavia, Y. et al. Doxorubicin-induced cardiomyopathy: From molecular mechanisms to therapeutic strategies. Journal of Molecular and Cellular Cardiology 52, 1213–1225 (2012).*
5. *McLaughlin, D. et al. Signalling mechanisms underlying doxorubicin and Nox2 NADPH oxidase-induced cardiomyopathy: involvement of mitofusin-2. British Journal of Pharmacology 174, 3677–3695 (2017).*
6. *L'Ecuyer, T. et al. DNA damage is an early event in doxorubicin-induced cardiac myocyte death. American Journal of Physiology-Heart and Circulatory Physiology 291, H1273–H1280 (2006).*
7. *Qiao, X. et al. Uncoupling DNA damage from chromatin damage to detoxify doxorubicin. PNAS 117, 15182–15192 (2020).*
8. *Marinello, J., Delcuratolo, M. & Capranico, G. Anthracyclines as Topoisomerase II Poisons: From Early Studies to New Perspectives. Int J Mol Sci 19, (2018).*
9. *Miller, K. D. et al. Cancer treatment and survivorship statistics, 2019. CA: A Cancer Journal for Clinicians 69, 363–385 (2019).*
10. *Kalani, M. Y. S. et al. Extracellular microRNAs in blood differentiate between ischaemic and haemorrhagic stroke subtypes. Journal of Extracellular Vesicles 9, 1713540 (2020).*
11. *Hoshino, A. et al. Tumour exosome integrins determine organotropic metastasis. Nature 527, 329–335 (2015).*
12. *Sancho-Albero, M. et al. Exosome origin determines cell targeting and the transfer of therapeutic nanoparticles towards target cells. J Nanobiotechnology 17, (2019).*
13. *Sanz-Rubio, D. et al. Stability of Circulating Exosomal miRNAs in Healthy Subjects. Sci Rep 8, 1–10 (2018).*
14. *Sulicka-Grodzicka, J. et al. Cranial Irradiation in Childhood Acute Lymphoblastic Leukemia Is Related to Subclinical Left Ventricular Dysfunction and Reduced Large Artery Compliance in Cancer Survivors. J Clin Med 8, (2019).*
15. *Théry, C. et al. Minimal information for studies of extracellular vesicles 2018 (MISEV2018): a position statement of the International Society for Extracellular Vesicles and update of the MISEV2014 guidelines. Journal of Extracellular Vesicles 7, 1535750 (2018).*
16. *Babraham Bioinformatics - FastQC A Quality Control tool for High Throughput Sequence Data. http://www.bioinformatics.babraham.ac.uk/projects/fastqc/.*
17. *Martin, M. Cutadapt removes adapter sequences from high-throughput sequencing reads. EMBnet.journal 17, 10–12 (2011).*

18. *Kozomara, A., Birgaoanu, M. & Griffiths-Jones, S. miRBase: from microRNA sequences to function. Nucleic Acids Res 47, D155–D162 (2019).*
19. *Friedländer, M. R., Mackowiak, S. D., Li, N., Chen, W. & Rajewsky, N. miRDeep2 accurately identifies known and hundreds of novel microRNA genes in seven animal clades. Nucleic Acids Res. 40, 37–52 (2012).*
20. *Dobin, A. et al. STAR: ultrafast universal RNA-seq aligner. Bioinformatics 29, 15–21 (2013).*
21. *Anders, S., Pyl, P. T. & Huber, W. HTSeq—a Python framework to work with high-throughput sequencing data. Bioinformatics 31, 166–169 (2015).*
22. *Wagner, N. et al. Coronary vessel development requires activation of the TrkB neurotrophin receptor by the Wilms' tumor transcription factor Wt1. Genes Dev. 19, 2631–2642 (2005).*
23. *Gutkind, J. S. & Offermanns, S. A New Gq-Initiated MAPK Signaling Pathway in the Heart. Developmental Cell 16, 163–164 (2009).*
24. *Goukassian, D., Morgan, J. & Yan, X. Neuregulin1-ErbB Signaling in Doxorubicin-Induced Cardiotoxicity. Cardiotoxicity of Oncologic Treatments (2012) doi:10.5772/33485.*
25. *Vasti, C. & Hertig, C. M. Neuregulin-1/erbB activities with focus on the susceptibility of the heart to anthracyclines. World J Cardiol 6, 653–662 (2014).*
26. *Fulgenzi, G. et al. BDNF modulates heart contraction force and long-term homeostasis through truncated TrkB.T1 receptor activation. J Cell Biol 210, 1003–1012 (2015).*
27. *Chen, Y. et al. Long Non-coding RNA ECRAR Triggers Post-natal Myocardial Regeneration by Activating ERK1/2 Signaling. Molecular Therapy 27, 29–45 (2019).*
28. *Funahashi, H. et al. Altered microRNA expression associated with reduced catecholamine sensitivity in patients with chronic heart failure. J Cardiol 57, 338–344 (2011).*
29. *Shah, S. et al. Genome-wide association and Mendelian randomisation analysis provide insights into the pathogenesis of heart failure. Nature Communications 11, 163 (2020).*
30. *Huan, T. et al. Genome-wide identification of microRNA expression quantitative trait loci. Nature Communications 6, 6601 (2015).*
31. *Tong, Z., Cui, Q., Wang, J. & Zhou, Y. TransmiR v2.0: an updated transcription factor-microRNA regulation database. Nucleic Acids Res 47, D253–D258 (2019).*
32. *Boehme, K. A., Kulikov, R. & Blattner, C. p53 stabilization in response to DNA damage requires Akt/PKB and DNA-PK. PNAS 105, 7785–7790 (2008).*
33. *Jain, S., Wei, J., Mitrani, L. R. & Bishopric, N. H. Auto-acetylation stabilizes p300 in cardiac myocytes during acute oxidative stress, promoting STAT3 accumulation and cell survival. Breast Cancer Res. Treat. 135, 103–114 (2012).*
34. *McSweeney, K. M., Bozza, W. P., Alterovitz, W.-L. & Zhang, B. Transcriptomic profiling reveals p53 as a key regulator of doxorubicin-induced cardiotoxicity. Cell Death Discov. 5, 1–11 (2019).*
35. *Fischer Andreas et al. Combined Loss of Hey1 and HeyL Causes Congenital Heart Defects Because of Impaired Epithelial to Mesenchymal Transition. Circulation Research 100, 856–863 (2007).*

36. *Lacher, S. E., Levings, D. C., Freeman, S. & Slattery, M. Identification of a functional antioxidant response element at the HIF1A locus. Redox Biology 19, 401–411 (2018).*
37. *Oyake, T. et al. Bach proteins belong to a novel family of BTB-basic leucine zipper transcription factors that interact with MafK and regulate transcription through the NF-E2 site. Molecular and Cellular Biology 16, 6083–6095 (1996).*
38. *Yang, Z. et al. Silencing of miR-193a-5p increases the chemosensitivity of prostate cancer cells to docetaxel. Journal of Experimental & Clinical Cancer Research 36, 178 (2017).*
39. *Shi, L. et al. MiR-141 Activates Nrf2-Dependent Antioxidant Pathway via Down-Regulating the Expression of Keap1 Conferring the Resistance of Hepatocellular Carcinoma Cells to 5-Fluorouracil. Cell. Physiol. Biochem. 35, 2333–2348 (2015).*
40. *Akat, K. M. et al. Comparative RNA-sequencing analysis of myocardial and circulating small RNAs in human heart failure and their utility as biomarkers. PNAS 111, 11151–11156 (2014).*
41. *Mertens, A. C. et al. Cause-Specific Late Mortality Among 5-Year Survivors of Childhood Cancer: The Childhood Cancer Survivor Study. J Natl Cancer Inst 100, 1368–1379 (2008).*
42. *Tukenova, M. et al. Role of Cancer Treatment in Long-Term Overall and Cardiovascular Mortality After Childhood Cancer. JCO 28, 1308–1315 (2010).*
43. *Crone, S. A. et al. ErbB2 is essential in the prevention of dilated cardiomyopathy. Nat. Med. 8, 459–465 (2002).*
44. *Benjanuwattra, J., Siri-Angkul, N., Chattipakorn, S. C. & Chattipakorn, N. Doxorubicin and its proarrhythmic effects: A comprehensive review of the evidence from experimental and clinical studies. Pharmacological Research 151, 104542 (2020).*
45. *Vandewalle, C. et al. SIP1/ZEB2 induces EMT by repressing genes of different epithelial cell–cell junctions. Nucleic Acids Res 33, 6566–6578 (2005).*
46. *Leong, K. G. et al. Jagged1-mediated Notch activation induces epithelial-to-mesenchymal transition through Slug-induced repression of E-cadherin. Journal of Experimental Medicine 204, 2935–2948 (2007).*
47. *Medici, D., Hay, E. D. & Olsen, B. R. Snail and Slug Promote Epithelial-Mesenchymal Transition through β-Catenin–T-Cell Factor-4-dependent Expression of Transforming Growth Factor-β3. Mol Biol Cell 19, 4875–4887 (2008).*
48. *Richter, A. et al. BMP4 promotes EMT and mesodermal commitment in human embryonic stem cells via SLUG and MSX2. Stem Cells 32, 636–648 (2014).*
49. *Pallier, K. et al. TWIST1 a New Determinant of Epithelial to Mesenchymal Transition in EGFR Mutated Lung Adenocarcinoma. PLOS ONE 7, e29954 (2012).*
50. *Zavadil, J., Cermak, L., Soto-Nieves, N. & Böttinger, E. P. Integration of TGF-beta/Smad and Jagged1/Notch signalling in epithelial-to-mesenchymal transition. EMBO J. 23, 1155–1165 (2004).*
51. *Ferrarelli, L. K. Revisiting TGF-β and EMT. Science 363, 941–943 (2019).*

52. *Tato-Costa, J. et al. Therapy-Induced Cellular Senescence Induces Epithelial-to-Mesenchymal Transition and Increases Invasiveness in Rectal Cancer. Clin Colorectal Cancer 15, 170-178.e3 (2016).*
53. *Kalluri, R. & Neilson, E. G. Epithelial-mesenchymal transition and its implications for fibrosis. J Clin Invest 112, 1776–1784 (2003).*
54. *Sun, H. et al. Nucleolin protects against doxorubicin-induced cardiotoxicity via upregulating microRNA-21. J. Cell. Physiol. 233, 9516–9525 (2018).*
55. *Soto-Gamez, A., Quax, W. J. & Demaria, M. Regulation of Survival Networks in Senescent Cells: From Mechanisms to Interventions. Journal of Molecular Biology 431, 2629–2643 (2019).*
56. *Baar, M. P. et al. Targeted Apoptosis of Senescent Cells Restores Tissue Homeostasis in Response to Chemotoxicity and Aging. Cell 169, 132-147.e16 (2017).*
57. *Demaria, M. et al. Cellular Senescence Promotes Adverse Effects of Chemotherapy and Cancer Relapse. Cancer Discov 7, 165–176 (2017).*
58. *Mancilla, T. A., Andrews, T. & Aune, G. Doxorubicin-Induced Chronic Upregulation of Transforming Growth Factor-beta. The FASEB Journal 30, 1205.6-1205.6 (2016).*
59. *Niessen, K. et al. Slug is a direct Notch target required for initiation of cardiac cushion cellularization. J Cell Biol 182, 315–325 (2008).*
60. *Vincentz, J. W. et al. Twist1 Controls a Cell-Specification Switch Governing Cell Fate Decisions within the Cardiac Neural Crest. PLoS Genet 9, (2013).*
61. *Min, Y.-L. et al. Identification of a multipotent Twist2-expressing cell population in the adult heart. PNAS 115, E8430–E8439 (2018).*
62. *Baumgarten, A. et al. TWIST1 regulates the activity of ubiquitin proteasome system via the miR-199/214 cluster in human end-stage dilated cardiomyopathy. International Journal of Cardiology 168, 1447–1452 (2013).*
63. *Paul, M. K. et al. Dynamic Changes in Intracellular ROS Levels Regulate Airway Basal Stem Cell Homeostasis through Nrf2-Dependent Notch Signaling. Cell Stem Cell 15, 199–214 (2014).*
64. *Martinez, E. C. et al. MicroRNA-31 promotes adverse cardiac remodeling and dysfunction in ischemic heart disease. J Mol Cell Cardiol 112, 27–39 (2017).*
65. *Gupta, S. K. et al. Quaking Inhibits Doxorubicin-Mediated Cardiotoxicity Through Regulation of Cardiac Circular RNA Expression. Circ. Res. 122, 246–254 (2018).*
66. *Li, S. et al. Nrf2 deficiency exaggerates doxorubicin-induced cardiotoxicity and cardiac dysfunction. Oxid Med Cell Longev 2014, 748524 (2014).*
67. *Nordgren, K. K. S. & Wallace, K. B. Disruption of the Keap1/Nrf2-Antioxidant Response System After Chronic Doxorubicin Exposure In Vivo. Cardiovasc Toxicol 20, 557–570 (2020).*
68. *Zhao, L. et al. MicroRNA-140-5p aggravates doxorubicin-induced cardiotoxicity by promoting myocardial oxidative stress via targeting Nrf2 and Sirt2. Redox Biol 15, 284–296 (2018).*

69. *Dreger, H. et al. Nrf2-dependent upregulation of antioxidative enzymes: a novel pathway for proteasome inhibitor-mediated cardioprotection. Cardiovasc. Res. 83, 354–361 (2009).*
70. *Gambino, V. et al. Oxidative stress activates a specific p53 transcriptional response that regulates cellular senescence and aging. Aging Cell 12, 435–445 (2013).*
71. *Hiebert, P. et al. Nrf2-Mediated Fibroblast Reprogramming Drives Cellular Senescence by Targeting the Matrisome. Developmental Cell 46, 145-161.e10 (2018).*
72. *Noguchi, Y.-T. et al. Cell-autonomous and redundant roles of Hey1 and HeyL in muscle stem cells: HeyL requires Hes1 to bind diverse DNA sites. Development 146, (2019).*
73. *Liu, L. et al. Impaired Notch Signaling Leads to a Decrease in p53 Activity and Mitotic Catastrophe in Aged Muscle Stem Cells. Cell Stem Cell 23, 544-556.e4 (2018).*
74. *Miao, L. et al. Notch signaling regulates Hey2 expression in a spatiotemporal dependent manner during cardiac morphogenesis and trabecular specification. Scientific Reports 8, 2678 (2018).*
75. *Sakata, Y. et al. Ventricular septal defect and cardiomyopathy in mice lacking the transcription factor CHF1/Hey2. Proc. Natl. Acad. Sci. U.S.A. 99, 16197–16202 (2002).*
76. *Xin, M. et al. Essential roles of the bHLH transcription factor Hrt2 in repression of atrial gene expression and maintenance of postnatal cardiac function. PNAS 104, 7975–7980 (2007).*
77. *Cieply, B. et al. Suppression of the epithelial-mesenchymal transition by Grainyhead-like-2. Cancer Res. 72, 2440–2453 (2012).*
78. *Wakabayashi, N. et al. Notch-Nrf2 Axis: Regulation of Nrf2 Gene Expression and Cytoprotection by Notch Signaling. Molecular and Cellular Biology 34, 653–663 (2014).*
79. *Yuan, Z. et al. Structural and Functional Studies of the RBPJ-SHARP Complex Reveal a Conserved Corepressor Binding Site. Cell Reports 26, 845-854.e6 (2019).*
80. *Steidl, C. et al. Characterization of the Human and Mouse HEY1, HEY2, and HEYL Genes: Cloning, Mapping, and Mutation Screening of a New bHLH Gene Family. Genomics 66, 195–203 (2000).*
81. *Chang, A. T. et al. An evolutionarily conserved DNA architecture determines target specificity of the TWIST family bHLH transcription factors. Genes Dev. 29, 603–616 (2015).*
82. *Jones, S. An overview of the basic helix-loop-helix proteins. Genome Biol 5, 226 (2004).*
83. *Yang, F., Kemp, C. J. & Henikoff, S. Anthracyclines induce double-strand DNA breaks at active gene promoters. Mutat Res 773, 9–15 (2015).*
84. *Awwad, S. W., Abu-Zhayia, E. R., Guttmann-Raviv, N. & Ayoub, N. NELF-E is recruited to DNA double-strand break sites to promote transcriptional repression and repair. EMBO reports 18, 745–764 (2017).*
85. *Jih, G. et al. Unique roles for histone H3K9me states in RNAi and heritable silencing of transcription. Nature 547, 463–467 (2017).*
86. *O'Hagan, H. M., Mohammad, H. P. & Baylin, S. B. Double strand breaks can initiate gene silencing and SIRT1-dependent onset of DNA methylation in an exogenous promoter CpG island. PLoS Genet. 4, e1000155 (2008).*

Figures

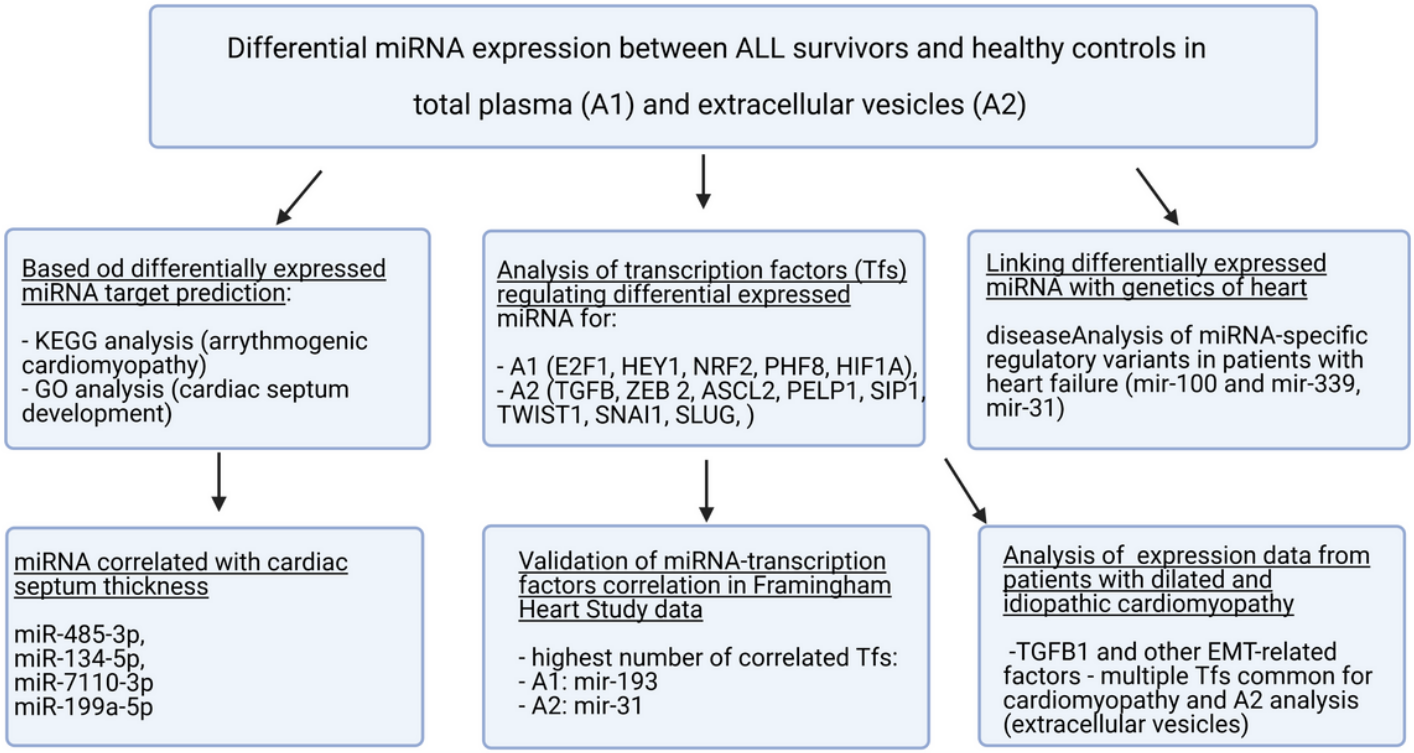

Figure 1

Summary of analysis performed and obtained results

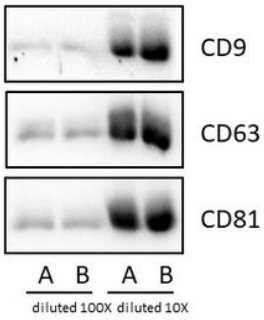

Figure 2

Western blot results for extracellular vesicles tested for presence o CD9, CD81, CD63.

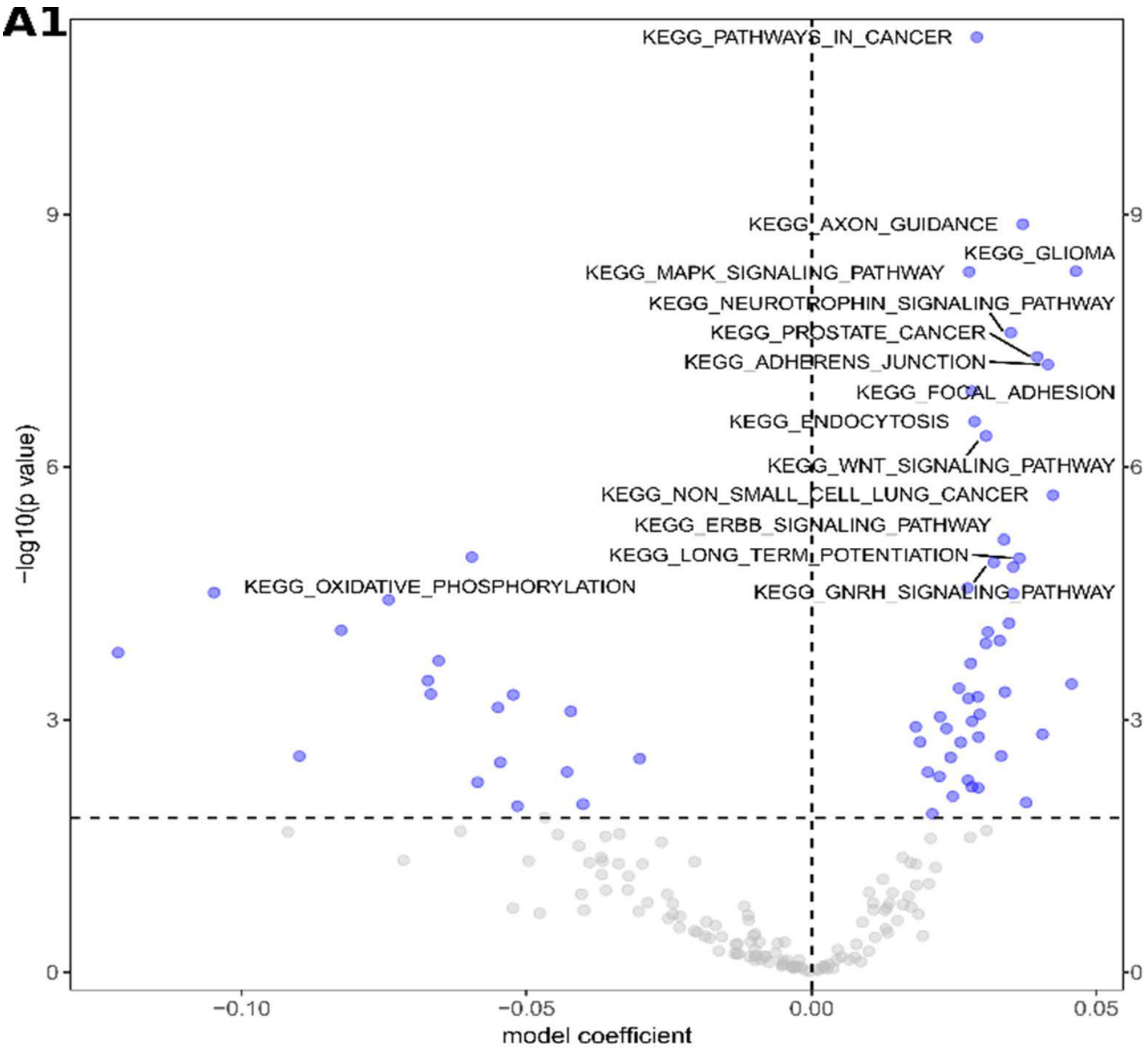

Figure 3

Pathways indicated by differentially expressed miRNA in total plasma (A1 analysis)

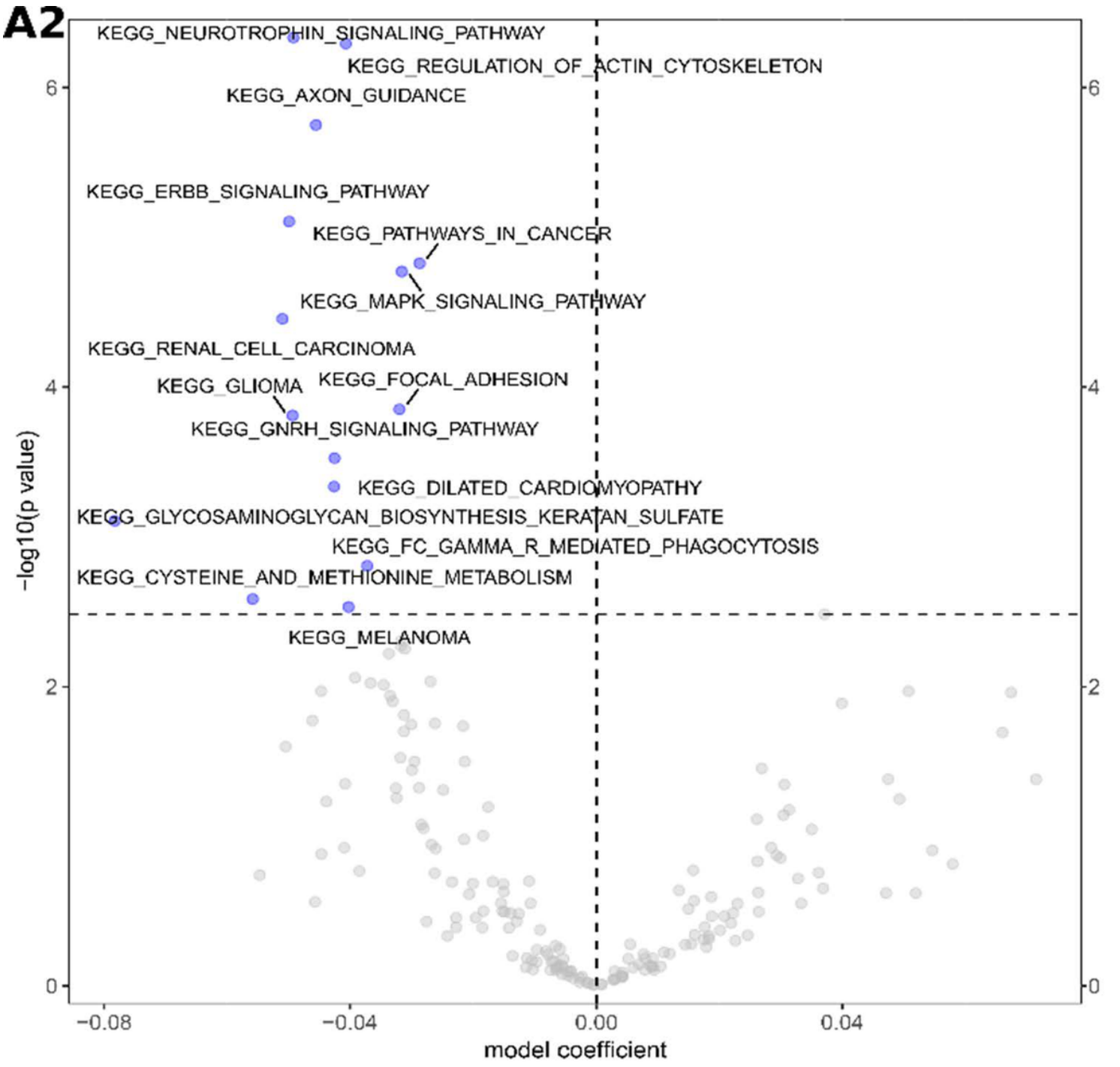

Figure 4

Pathways indicated by differentially expressed miRNA in extracellular vesicles (A2 analysis)

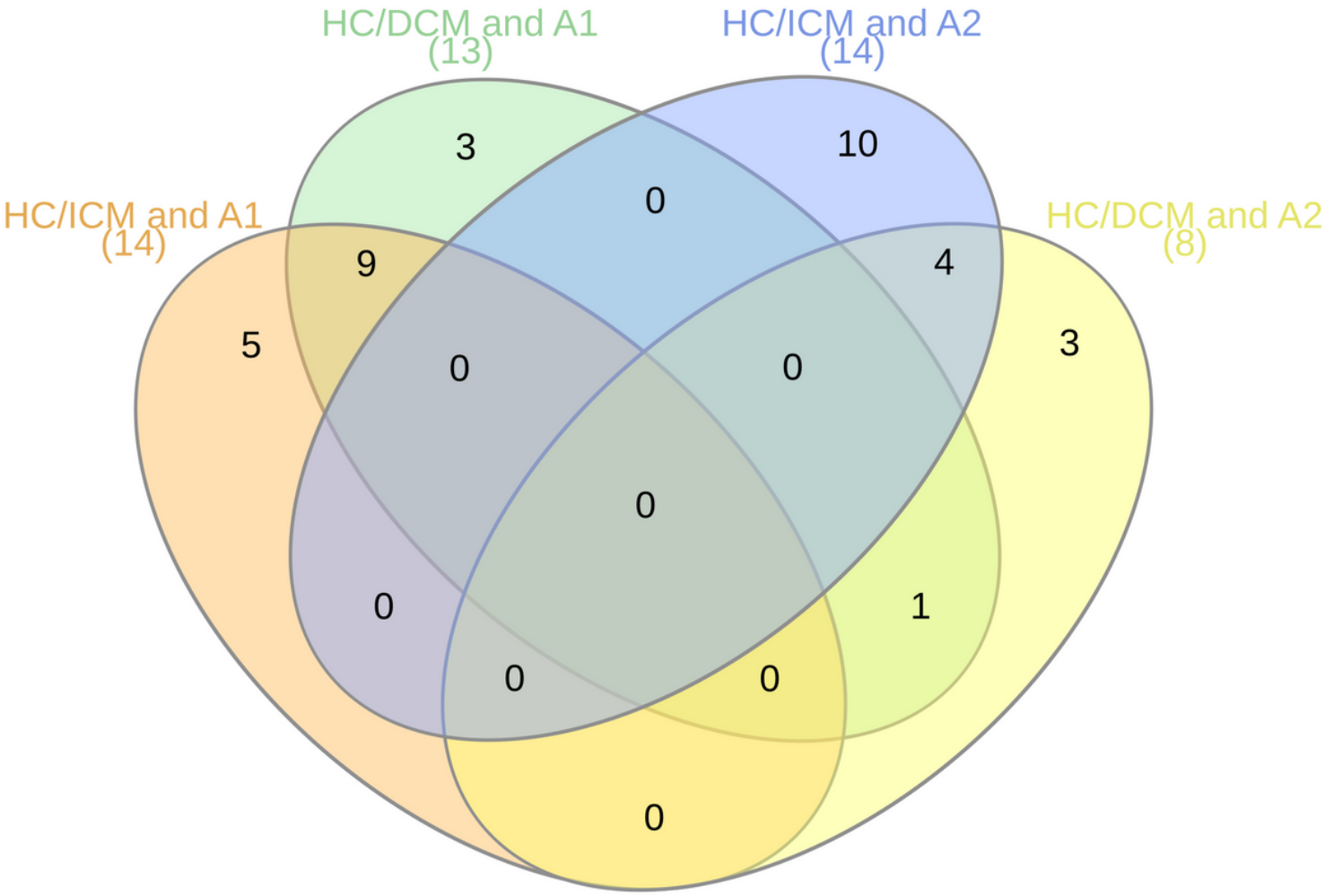

Figure 5

Comparison of A1 and A2 analyses with results of differential expression of circulating miRNA data from patients with idiopathic cardiomyopathy (ICM) or dilated cardiomyopathy (DCM) compared to healthy individuals (HC).

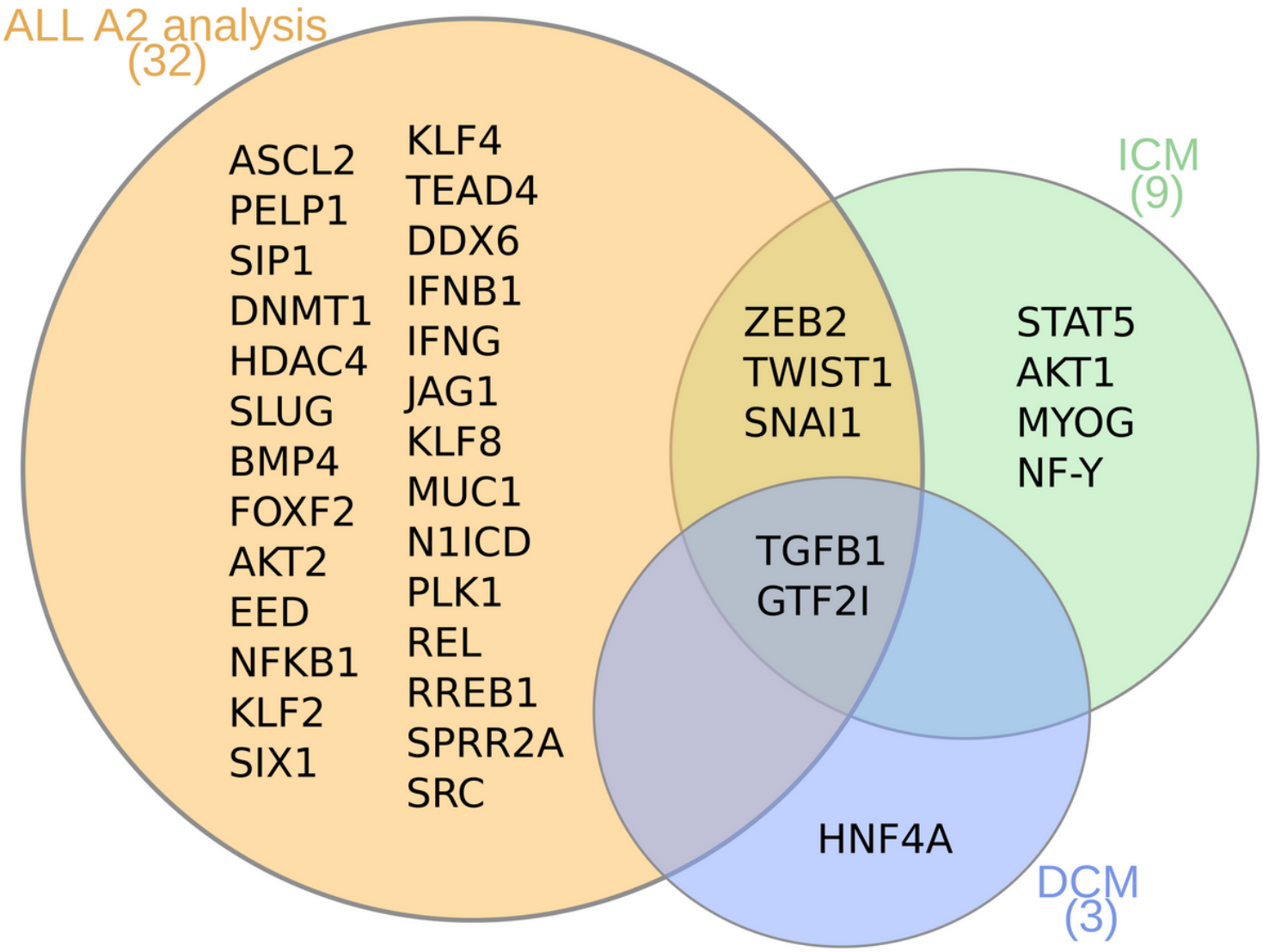

Figure 6

Comparison of transcription factors regulating ICM and DCM datasets with transcription factors regulating expression of miRNA in A1 and A2 analyses.

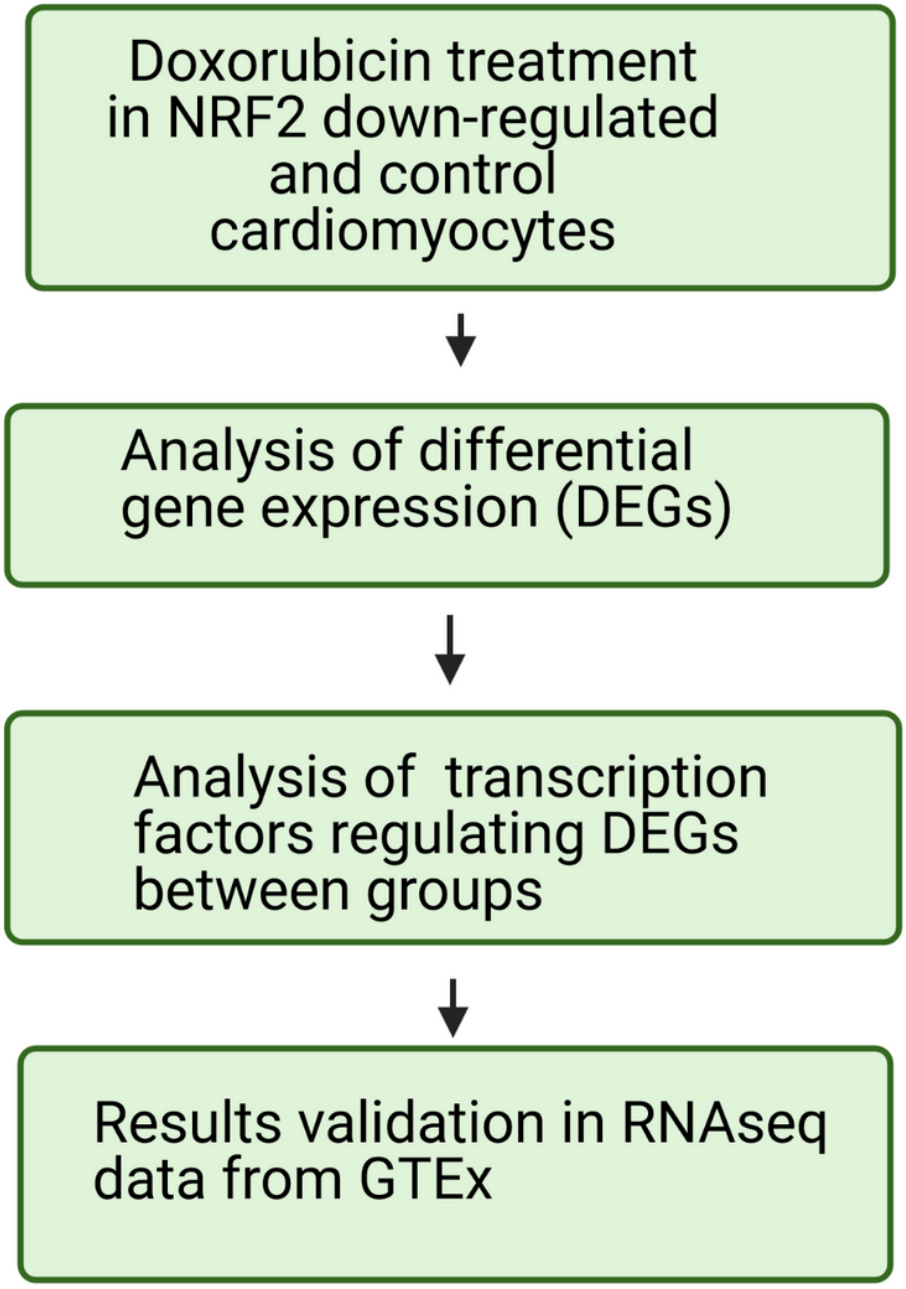

Figure 7

Graphical summary of analytical steps performed on RNA-seq data from culture cardiomyocytes treated with doxorubicin and with down-regulated NRF2.

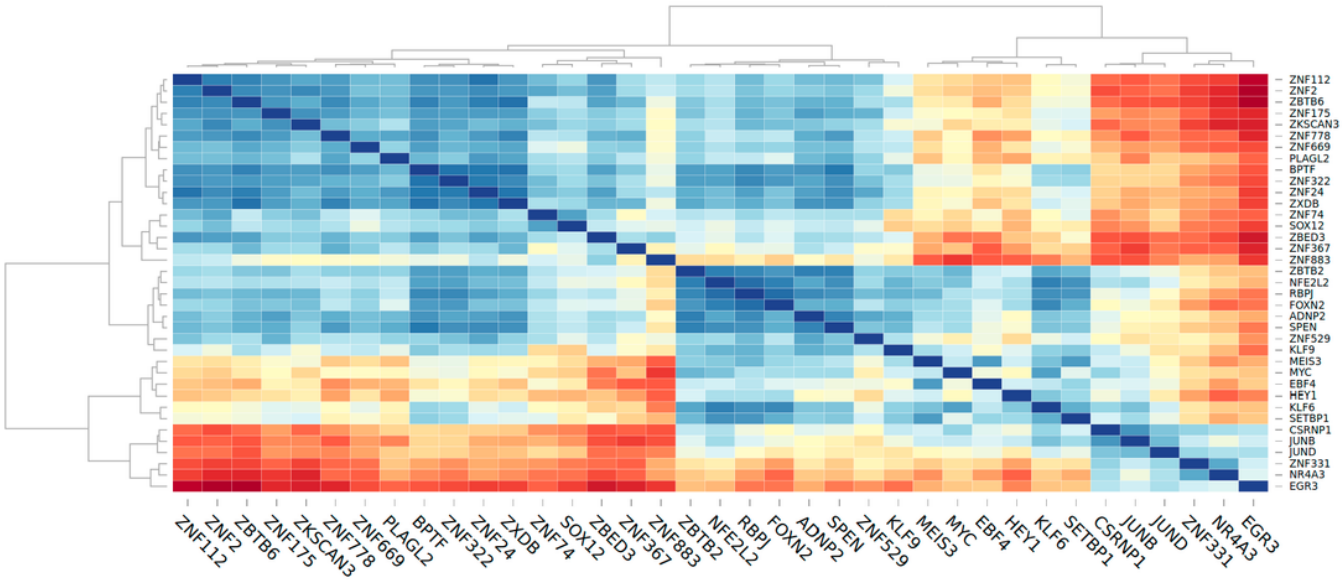

Figure 8

Heatmap plots of co-expression of NRF2 with selected TFs in GTEx Heart Left Ventricle RNA-sequencing data for T1 subset.

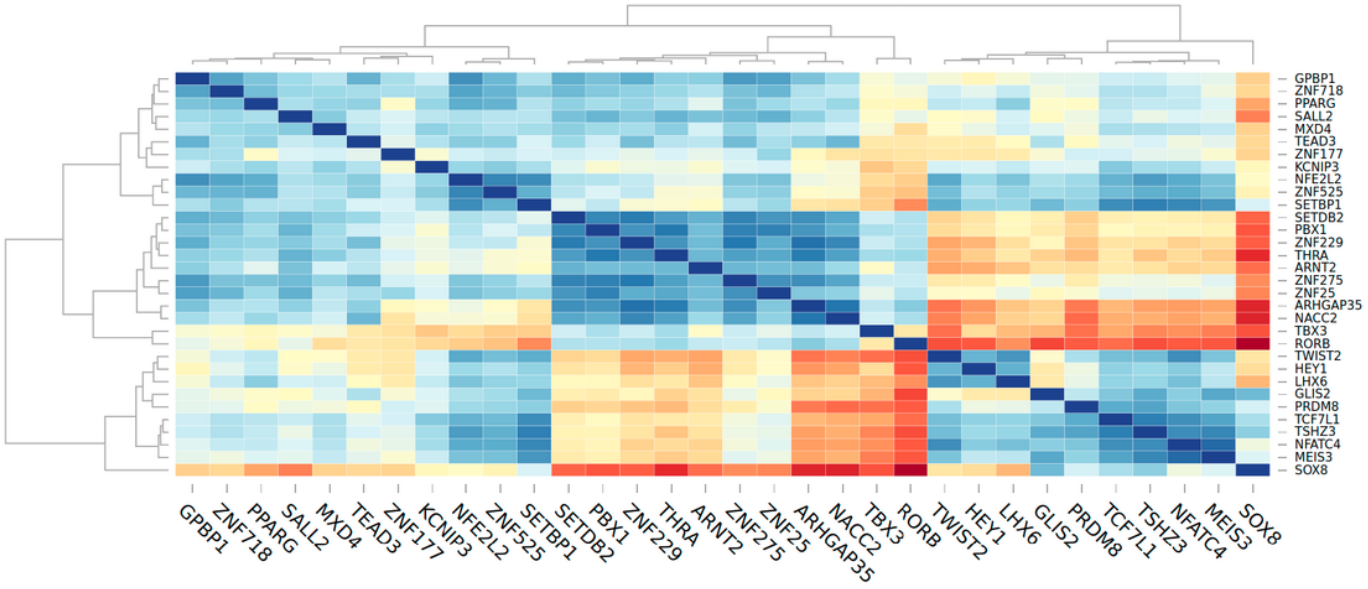

Figure 9

Heatmap plots of co-expression of NRF2 with selected TFs in GTEx Heart Left Ventricle RNA-sequencing data for T2 subset.

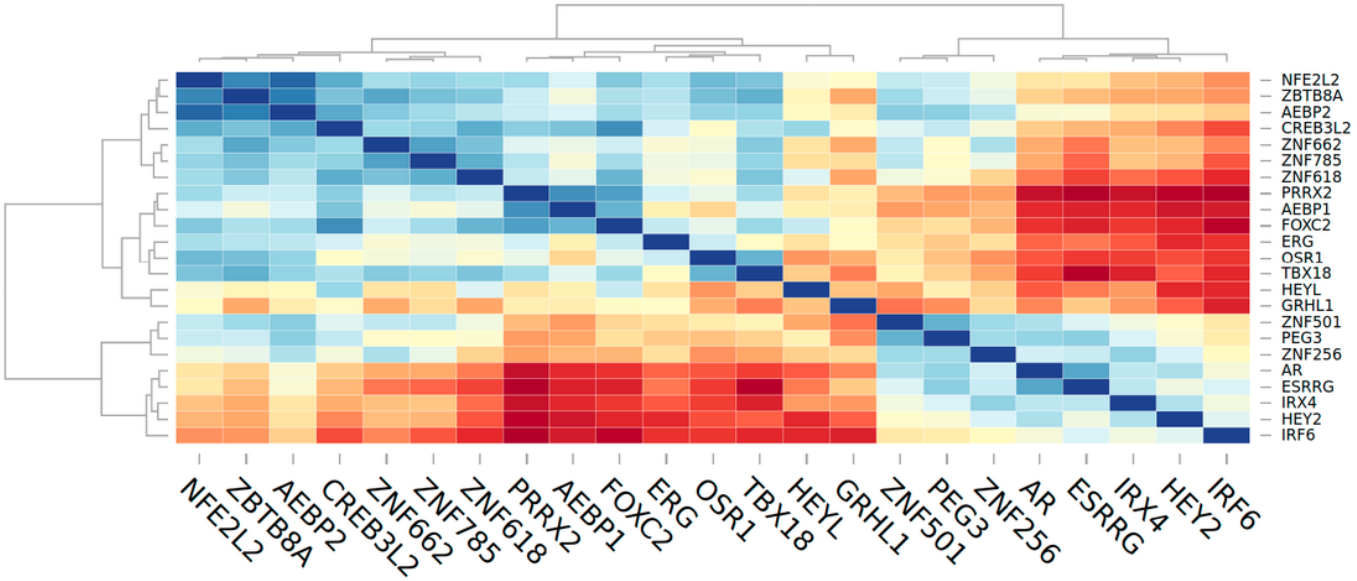

Figure 10

Heatmap plots of co-expression of NRF2 with selected TFs in GTEx Heart Left Ventricle RNA-sequencing data for T3 subset.

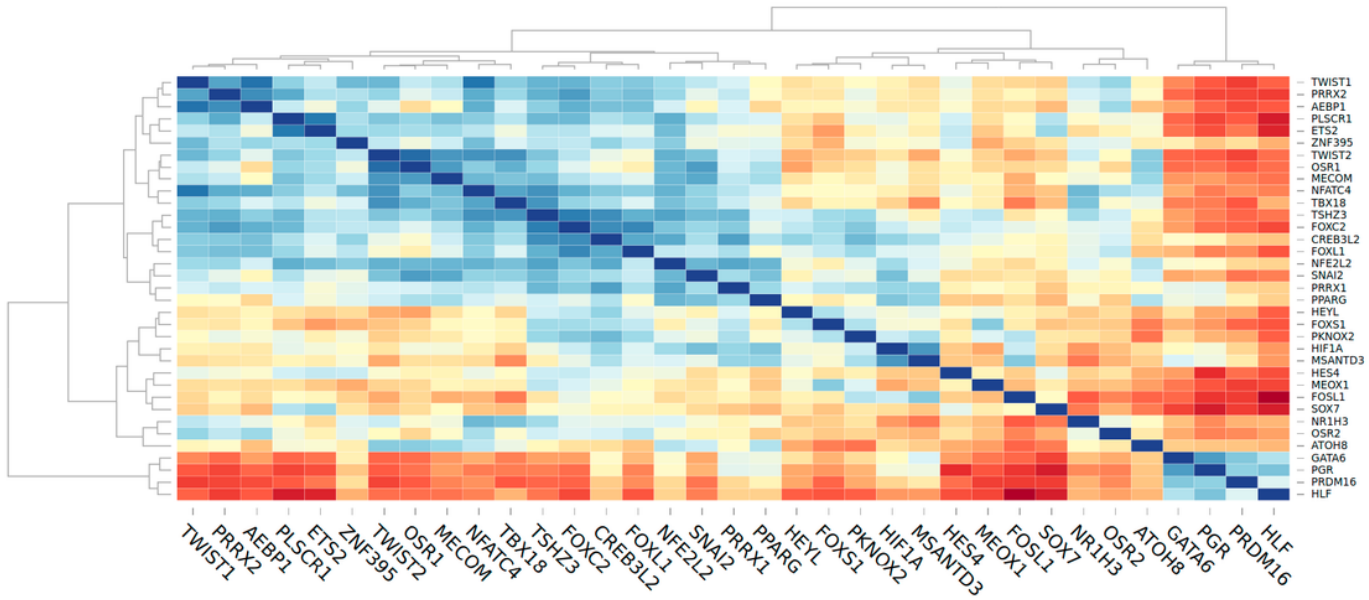

Figure 11

Heatmap plots of co-expression of NRF2 with selected TFs in GTEx Heart Left Ventricle RNA-sequencing data for T4 subset.

Supplementary Files

This is a list of supplementary files associated with this preprint. Click to download.

- SupplementaryScientificReports.pdf